Gondwana Research 24 (2013) 902–917

Contents lists available at ScienceDirect

Gondwana Research

journal homepage: www.elsevier.com/locate/gr

Systematic variations in seismic velocity and reflection in the crust of Cathaysia: New constraints on intraplate orogeny in the South China continent

Zhongjie Zhang [a,*], Tao Xu [a], Bing Zhao [a], José Badal [b]

[a] State Key Laboratory of Lithospheric Evolution, Institute of Geology and Geophysics, Chinese Academy of Sciences, Beijing 100029, China
[b] Physics of the Earth, Sciences B, University of Zaragoza, Pedro Cerbuna 12, 50009 Zaragoza, Spain

ARTICLE INFO

Article history:
Received 16 December 2011
Received in revised form 15 May 2012
Accepted 18 May 2012
Available online 18 June 2012

Keywords:
Wide-angle seismic data
Crustal velocity
Frequency filtering
Migration and stacking
Lithospheric extension
Yangtze block
Cathaysia block

ABSTRACT

The South China continent has a Mesozoic intraplate orogeny in its interior and an oceanward younging in postorogenic magmatic activity. In order to determine the constraints afforded by deep structure on the formation of these characteristics, we reevaluate the distribution of crustal velocities and wide-angle seismic reflections in a 400 km-long wide-angle seismic profile between Lianxian, near Hunan Province, and Gangkou Island, near Guangzhou City, South China. The results demonstrate that to the east of the Chenzhou-Linwu Fault (CLF) (the southern segment of the Jiangshan–Shaoxing Fault), the thickness and average P-wave velocity both of the sedimentary layer and the crystalline basement display abrupt lateral variations, in contrast to layering to the west of the fault. This suggests that the deformation is well developed in the whole of the crust beneath the Cathaysia block, in agreement with seismic evidence on the eastwards migration of the orogeny and the development of a vast magmatic province. Further evidence of this phenomenon is provided in the systematic increases in seismic reflection strength from the Moho eastwards away from the boundary of the CLF, as revealed by multi-filtered (with band-pass frequency range of 1–4, 1–8, 1–12 and 1–16 Hz) wide-angle seismic images through pre-stack migration in the depth domain, and in the P-wave velocity model obtained by travel time fitting. The CLF itself penetrates with a dip angle of about 22° to the bottom of the middle part of the crust, and then penetrates with a dip angle of less than 17° in the lower crust. The systematic variation in seismic velocity, reflection strength and discrepancy of extensional factors between the crust and the lithosphere, are interpreted to be the seismic signature of the magmatic activity in the interest area, most likely caused by the intrusion of magma into the deep crust by lithospheric extension or mantle extrusion.

1. Introduction

The South China continent is located alongside the western margin of the Pacific plate, and has endured the subduction of this plate beneath mainland China (Grabau, 1924; Huang, 1980; Guo et al., 1983; Yang et al., 1986; Yin and Nie, 1993; Zhang et al., 1994). This region includes the Huanan fold belt, where a significant occurrence of Jurassic–Cretaceous postorogenic magmatism makes up a broad extension to the northeast (Li and Li, 2007). Late Mesozoic magmatic rocks, composed mostly of granite and rhyolite, outcrop at the surface, and are spread over a large area, making up 95% of a belt 600 km wide that lies along the southeastern coastline of China (Wang et al., 2003) (Fig. 1). Throughout the continent, volcanic rocks exist mainly to the east of the Chenzhou-Linwu Fault (CLF) or the southern segment of the Jiangshan–Shaoxing Fault. The CLF lies at a distance of about 450 km from the belt. The igneous rocks found in South China fall into three main age groups, namely early (180–160 Ma), mid (160–140 Ma) and late (140–97 Ma) Yanshanian (Wang et al., 2003). In some areas, the late Yanshanian group includes rocks as young as ca. 79 Ma (Martin et al., 1994). The early Yanshanian volcanism belongs to a K-rich calc-alkaline series inter-layered with other rocks or shallow-water detrital materials. In contrast, the late Yanshanian volcanism has a bimodal character associated with the continental red beds that lie along grabens that trend NE–SW, and indicate intraplate rifting. Granitoids are found in a great variety of petrographic types from biotite–granite to tonalite. Peraluminous granitoids formed by crustal melting are also common (Jahn et al., 1990). Outcrops of volcanic rock become more common nearer the ocean (Zeng et al., 1997; Zhou and Li, 2000; Wang et al., 2003). Li and Li (2007) divided the synorogenic magmatism into three age groups, 230–210, 240–230 and 280–240 Ma, and the postorogenic magmatism into four age groups, namely 120–80, 145–120, 170–145, and 195–170 Ma. The exact character of the intraplate orogeny and the extensive postorogenic magmatism are still the subject of considerable debate.

In the last 20 years, a number of tectonic models have been postulated to account for the Mesozoic tectonic evolution of the South China block (Jahn et al., 1986; Hsü et al., 1988; Rodgers, 1989; Rowley et al., 1989; Jahn et al., 1990; Charvet et al., 1996; Li et al., 2000; Zhou and

* Corresponding author.
E-mail addresses: zhangzj@mail.iggcas.ac.cn (Z. Zhang), badal@unizar.es (J. Badal).

1342-937X/$ – see front matter
http://dx.doi.org/10.1016/j.gr.2012.05.018

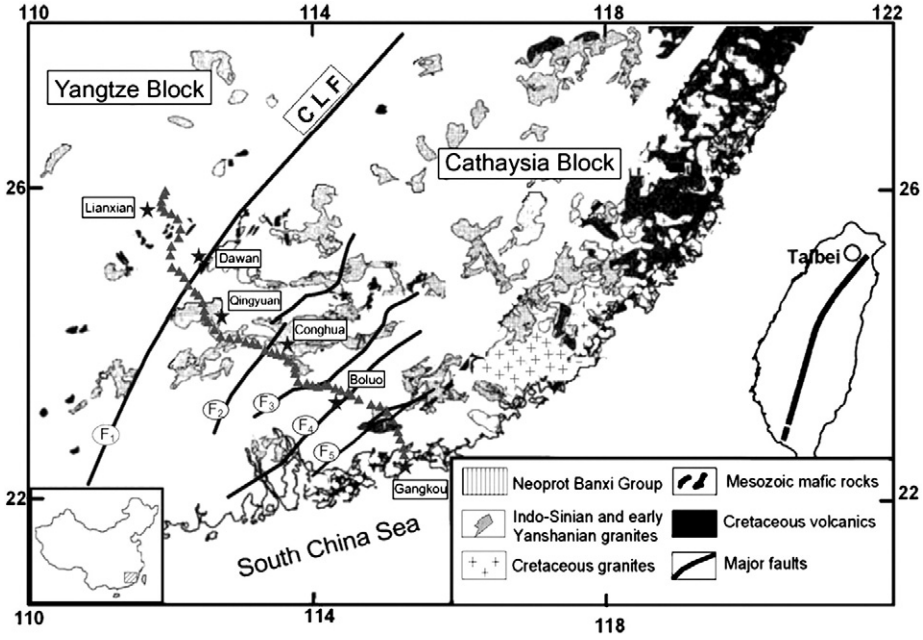

Fig. 1. Location map showing the wide-angle seismic profile from northwest to southeast between Lianxian and Gangkou Island. The triangles and stars respectively mark the geographical positions of the stations and shot points (Lianxian, Dawan, Qingyuan, Conghua, Boluo and Gangkou). The major active faults that cross the seismic profile almost perpendicularly are: F1, Chenzhou-Linwu fault; F2, Enping-Xinfeng fault; F3, Heyuan-Zengcheng fault; F4, Zijjin-Boluo fault; F5, Lianhuashan fault. The inset at the bottom left shows the study region and the extent of the South China fold belt. The classification of the regional magmatism is also shown by geological age (bottom of figure).

Li, 2000; Wang et al., 2003). These models include an Andean-type active continental margin (Guo et al., 1983), an Alpine-type collision belt (Hsü et al., 1988, 1990), and lithospheric subduction (Holloway, 1982; Faure, 1996; Zhou and Li, 2000) with an underplating of mafic magma (Li and Li, 2007); all these models suppose that the tectonic regime was dominantly compressive as a result of either a westward subduction of a Mesozoic Pacific plate, or the closure of an oceanic basin in the interior of the South China block (Holloway, 1982; Hsü et al., 1990; Faure, 1996; Zhou and Li, 2000). Other alternative models include wrench faulting (Xu et al., 1993), continental rifting and extension (Gilder et al., 1996; Li et al., 2000; Wang et al., 2003) and a flat-slab subduction model (Li and Li, 2007); these models differ from the previous because they suggest that intraplate lithospheric extension and thinning have been dominant since the overthrusting tectonics that took place during the Early Mesozoic in south China (Li et al., 1989; Faure, 1996; Gilder et al., 1996; Li et al., 2000; Wang et al., 2003; Li and Li, 2007). All these tectonic models have been proposed in reference to the tectonics and the data on surface geology and geochemistry, but they must all be tightly constrained by the seismic structure of the crust and uppermost mantle.

With the intention of providing a broader view on this issue, and of contributing to our understanding of the intraplate tectonics of Asia through seismology, based on the seismic response of the crust in the frame of the Mesozoic tectonic evolution, we have constructed a set of wide-angle seismic reflection sections by taking advantage of the high quality data provided by an active source experiment consisting of a 400-km-long seismic profile (Fig. 1). Even though the contact relationship between the Cathaysia and the Yangtze blocks with reference to crustal P-wave velocity model has previously been described (Zhang and Wang, 2007), the geometry of the fault is still unclear, and this is important if we are to understand the intraplate deformation. To that end we herein reevaluate the crustal P-wave velocity distribution (Zhang and Wang, 2007) and pre-stack migrated wide-angle seismic reflections (Milkereit, 1987; Milkereit et al., 1990; Lafond and Levander, 1995; Zhang et al., 2000).

The remainder of the paper is organized as follows: (1) we provide a brief picture of the tectonic setting of the study region probed by wide-angle seismic profiling; (2) we give a short description of the seismic dataset and its multi-filtered processing; (3) we describe the crustal P-velocity model used when implementing the working method, beginning with the application of a pre-stack migration scheme; (4) we discuss the reconstruction of seismic reflection sections in a multi-frequency band; (5) finally, we provide a discussion focused on the crustal response prior to the Mesozoic tectonic evolution.

2. Tectonic setting

Li and McCulloch (1996) declared that both the Yangtze and Cathaysia blocks were consolidated at ca. 970 Ma based on geological mapping of the tectonics of South China. In fact, a number of authors have shown that the Yangtze and Cathaysia blocks were consolidated during the Neoproterozoic rather than at ca. 970 Ma (e.g., Li et al., 1995, 2000, 2002a, 2002b; Zhou et al., 2002; Li et al., 2003, 2005; Greentree et al., 2006; Li et al., 2008; Wang et al., 2012). In recent years, the Neoproterozoic amalgamation of the Yangtze and Cathaysia Blocks is a hotly debated issue, with three viewpoints having been proposed. The first view involves amalgamation ages of (1) ca. 880 Ma (e.g., Li et al., 1995, 2002a, 2002b; Greentree et al., 2006; Li et al., 2008), (2) ca. 830 Ma (e.g., Li et al., 2002a, 2002b, 2003, 2005), and (3) ca. 800 Ma (e.g., Zhou et al., 2002). In the second view, the Cathaysia basement was traditionally considered to be characterized by the Paleoproterozoic Badou, Mayuan, Yunkai and Zhoutan Groups exposed mainly along Wuyi–Nanling–Yunkai domains (e.g., Li et al., 1989). However, the latest geochronological data show that these metamorphic rocks, which had previously been mapped as the Paleoproterozoic basement, and in particular the migmatite and gneissoid granites, have a wide range of ages from 410 to 1890 Ma (e.g., Wang et al., 2004, 2005, 2007, 2010, 2011).

The crystalline basement of the Yangtze block has an average age of 2.7–2.8 Ga (Qiu et al., 2000), with the oldest materials having an age of more than 3.2 Ga. In contrast, the crystalline basement of the Cathaysia block is made up of Paleo-to-Mesoproterozoic and possibly Late Archean rocks of about 2.5 Ga (Chen and Jahn, 1998; Wang et al., 2003).

Late Mesozoic magmatic rocks composed predominantly of granite and rhyolite are spread across a 600 km-long belt along the southeastern coastline of China, and form outcrops over 95% of the total exposed area

(Wang et al., 2003). Throughout the continent, Cretaceous volcanic rocks extend mainly over the eastern side of the Chenzhou-Linwu Fault (CLF), with the western boundary of this volcanic belt being located about 450 km away from the coast (Fig. 1). According to the distribution of the age of the Permian–Early Cretaceous magmatic material found along the wide-angle seismic profile, the rocks can be sorted into two age groups: the first includes rocks aged <195 Ma and the second includes rocks aged >210 Ma (Fig. 1). With respect to the latter group, the rocks are younger further inland, and further away from the continental margin. Regarding the former group, gradually younger rocks can be observed from the CLF towards South China and the coastline. To the northwest of the CLF, the young rocks have ages between 152 and 175 Ma, while to the southeast of this fault these ages range from about 190 to 122 Ma.

The South China tectonic setting consists of three main elements: the southeastern continental margin of the Yangtze block, the northwest continental margin of Cathaysia and the Chenzhou-Linwu Fault (CLF) or the southern segment of Jiangshan–Shaoxing Fault belt (Zhang et al., 1984; Angelier, 1990; Hou and Li, 1993; Duan et al., 2011). The Jiangshan–Shaoxing Fault extends from Jiangshan through Shaoxing to Pingxiang for a strike length of over 500 km. It has been widely considered to be the boundary fault or suture that was formed between the Yangtze and Cathaysia Blocks during their amalgamation in the early Neoproterozoic, giving rise to the coherent South China block (SCB). However, two different views exist concerning its southwestward extension. The first considers that it extends along the eastern margin of the Jiangnan-Xuefeng Domain. The second suggests that its southwestern segment can be defined by the Chenzhou-Linwu Fault that extends from Yongxing and Chenzhou (eastern Hunan) through Cengxi (eastern Guangxi) and Bobai (eastern Guangxi), thence into the Indochina Block. The Lianxian–Gangkou (LG) seismic profile crosses the Cathaysia block, the CLF and the southeastern margin of the Yangtze block from northwest to southeast (Fig. 1), thereby providing an excellent opportunity to understand the crustal response before the Mesozoic tectonic evolution of the region and their consequences, such as the difference in the magmatic activity observed between the Yangtze and Cathaysia blocks. The major active faults intersected by the seismic profile include: (1) the Chengzhou-Linwu fault (CLF, previously termed the Wuchuan-Sihui fault by Zhang and Wang, 2007) (F1), the Enping-Xinfeng fault (F2), the Heyuan-Zengcheng fault (F3), the Zijjin-Boluo fault (F4) and the Lianhuashan fault (F5). By checking age data from Dawan, in Yongxing (Chenzhou), just along the Chenzhou-Linwu Fault, it may be seen that the CLF or Wuchuang-Sihui Fault was originally defined as being located to the east of the Yunkai terrane, with an affinity for the Cathaysia Block. In fact, the southward extension of the Chenzhou-Linwu Fault in Hunan Province is locally known as the Bobai-Cengxi Fault/Linshan Fault in Guangxi. Even though the CL fault is proposed to be the boundary between the Cathaysia and the Yangtze blocks from the crustal velocity model, more complementary constraints are nevertheless needed to assess the arguments relating to the foregoing models and to understand the Mesozoic deformation from the intraplate orogeny.

3. Multi-filtered wide-angle data, crustal velocity and prestack migration scheme

3.1. Multi-filtered wide-angle seismic data

The results and interpretation of the wide-angle deep seismic sounding between Lianxian and Gangkou, conducted by the CAS Institute of Geophysics, and which was designed to determine the structure of the crust and upper mantle, are documented in detail by Li (1992), Yin et al. (1999) and Zhang and Wang (2007), among others. Here, we simply list some of the key results of this seismic experiment. The 400-km-long seismic profile whose azimuth lies at about N30°W runs from Lianxian, near Hunan Province, to Gangkou Island, near Guangzhou City, and intersects a series of NE faults, namely Chengzhou-Linwu, Enping-Xinfeng, Heyuan-Zengcheng, Zijjin-Boluo and Lianhuashan, respectively labeled F1 to F5 in Fig. 1 (Huang, 1980; Wang et al., 2003). Recording instruments consisting of three-component DZSS-1 seismographs were deployed along the profile and a total of six shots were fired at the sites of Lianxian, Dawan, Qingyuan, Conghua, Boluo and Gangkou (Fig. 1).

The seismic signals recorded by the seismographs were initially sampled at a rate of 2.5 ms, which guarantees the acquisition of data at the maximum frequency of 200 Hz (Nyquist frequency), even though wide-angle seismic transects usually consist of low-frequency records. Amplitude–frequency spectra obtained from P-wave seismic gathers at the six shot points range within the 1–20 Hz frequency interval (Fig. 2). We have filtered the set of seismic signals using four band-pass filters with frequencies of 1–4, 1–8, 1–12 and 1–16 Hz, thereby yielding 24 common shot gathers, four for each of the original gathers. Fig. 3b shows these filtered P-wave gathers with a reduced time scale using a reduction velocity of 6.0 km/s.

Regardless of the frequency band, all the seismograms show a high signal-to-noise ratio for Pg arrivals refracted above the crystalline basement and all show Pm (or PmP) waves reflected from the Moho with strong amplitudes. Pn-phases or head waves refracted along the Moho can be identified even though their amplitudes are small compared with those of the reflected phases on the Moho. The maximum offset for Pg events is 40–60 km on all common shot gathers, which is about 20–40 km shorter than in other places in South China (Zhang et al., 2005). This may be a result of the laterally varying composition of the sedimentary cover in South China (Zhang et al., 2008), or may be due to crustal deformation of different strengths (Gao et al., 2009; Zhang et al., 2009a,b). The variations in the arrival times of the frequency-filtered seismic events Pg, Pm and the other intracrustal reflections P1–P4 are not that great, but their respective strengths, especially those of the reflections from the Moho, show a strong dependence on the frequency band.

3.2. P-wave velocity model

The crustal P-velocity model used when implementing the pre-stack migration of wide-angle seismic data is shown in Fig. 4. This model allows us to show the upper, middle, and lower crust, the Moho discontinuity and the uppermost mantle for the LG transect (Zhang and Wang, 2007). The most significant details are: (1) the average thickness of the crust is about 34 km beneath the Yangtze block, and this gradually reduces from northwest to southeast beneath the Cathaysia block, especially in the middle segment of the profile, where it falls to 33 km. (2) The average P-wave velocity is about 6.3 km/s for the crust as a whole. (3) The apparent P-wave velocity of event P3 is slower than that of event P2. This finding suggests the possibility of a low velocity layer constrained by reflectors P2 and P3, although the existence of this low velocity layer cannot be fully confirmed because of the limitations of the field experiment. In our final model, there is a relatively narrow low-velocity layer with a thickness of about 5 km and a P-velocity of 5.8 km/s. (4) The crustal layers from the surface down to the Moho cease to be horizontal just at the point at which they cross the CLF in a southeasterly direction, a characteristic that continues at depth with a slope of around 17–22° or even less, and this suggests that this fault is the natural border between the Yangtze and Cathaysia blocks. (5) It is also worth noting that the penetration of the CLF seems to reach the Moho, a fact also supported by geochemical evidence (Wang et al., 2003).

3.3. Pre-stack migration of wide-angle seismic data

We have used pre-stack migration in the depth domain, and diffraction-stack migration (Milkereit, 1987; Milkereit et al., 1990; Lafond and Levander, 1995; Zhang et al., 2000) to reconstruct the fine structure of the crust and upper mantle. Phinney and Jurdy (1979),

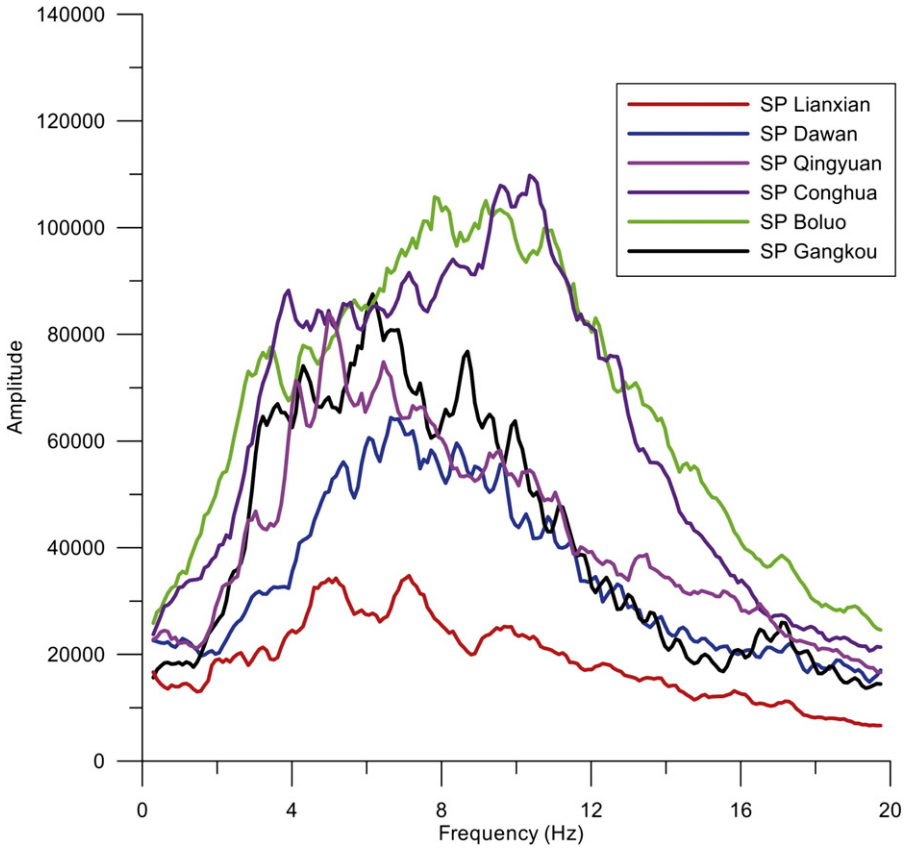

Fig. 2. Amplitude–frequency spectra obtained from six common shot gathers at Lianxian, Dawan, Qingyuan, Conghua, Boluo and Gangkou Island, South China (Fig. 1), showing the spectral content between 1 and 20 Hz.

Zhang et al. (2000) and van Avendonk Harm (2004) previously used slanting stacks of common-source gathers from wide-angle CMP profiles to back-project reflection energy to the subsurface. The stacking results for individual gathers form a complete image. Milkereit (1987) divided wide-angle profiles into overlapping, narrow-aperture spatial windows, and then used the appearance of localized slanting stacks in those windows to identify coherent arrivals in the time-distance domain, with the purpose of using these as inputs for diffraction-stack migration. Using this approach, contributions to the migrated image are restricted to input samples that arrive with travel times and ray parameters predicted for diffraction through a velocity model. This improves the spatial resolution by suppressing contributions from undesirable coherent noise. Any of these earlier approaches is capable of handling diffracted waves. The structure is brought into focus by summing the contributions from many overlapping source–receiver pairs. In essence, the pre-stack migration scheme involves three steps, namely (1) calculation of the travel times from the source to the imaging point and from the imaging point to the receiver using a finite-difference eikonal solver (Vidale, 1988; Zhao et al., 2004), and summing these two times; (2) migration of the seismic signal to the imaging point, bearing in mind the shot-to-receiver travel time; (3) assessment of the seismic amplitude of each imaging point to obtain the wide-angle seismic reflection structure of the crust (Phinney and Jurdy, 1979; Zhang et al., 2000; van Avendonk Harm, 2004).

4. Frequency-dependent seismic reflectivity images

To determine the structure of the seismic reflection of the crust, we first filtered the acquired data using band-pass filters of frequencies 1–4, 1–8, 1–12, and 1–16 Hz. We then made an inverse transformation into the time domain to obtain the corresponding wide-angle seismic sections for the different frequency ranges. Having done this, we followed the pre-stack migration scheme of the filtered seismic data using the previous P-velocity model (Fig. 4) in order to reconstruct the seismic reflectivity images of the crust and upper mantle. In this process the depth range of the model (0 km at the surface and 40 km at the Moho) was extended down as far as 60 km. At mantle depths beneath the Moho, we assumed that the P-velocity was constant (8.06 km/s). Lastly, a 1.5×1.5 km partition of the medium was used for implementation of wide-angle pre-stack migration.

Fig. 5 shows the seismic reflectivity images of the crust and uppermost mantle along the LG transect, which we obtained from pre-stack migration of wide-angle seismic data that had previously been filtered within the frequency ranges indicated above. These images show the changes in amplitude and phase of some reflection events in response to the frequency ranges considered herein; it may be seen that there are several events with relatively large amplitudes, and two of these are of particular interest. The first is at a depth of about 15 km and corresponds to seismic reflection on the bottom of the upper crust (P1), and the second is at a depth range within 33–35 km, corresponding to the P-wave reflected from the Moho (PmP).

The reflection coefficient associated with the Moho is large, which may suggest that there is not much partial melt in the lower crust, given that a partial melt zone would attenuate seismic energy. Nevertheless, multiple refracted Pn-phases are recorded after Pm arrivals, as can be seen from the shot fired at Dawan (Pn and Pn1 in Fig. 3a). The variability and complexity of these Pn events could either be due to the mantle topography that might lead to irregular scattering from the Moho interface (Zhang et al., 2000), or due to the stochastic structure underlying the Moho (Poppeliers and Levander, 2004). In our case, there could be an uneven topography of the crust–mantle boundary, such as an abrupt discontinuity of velocity, or else a transition zone accentuated by a strong velocity gradient (Zhang et al., 2000; Lin and Wang, 2005).

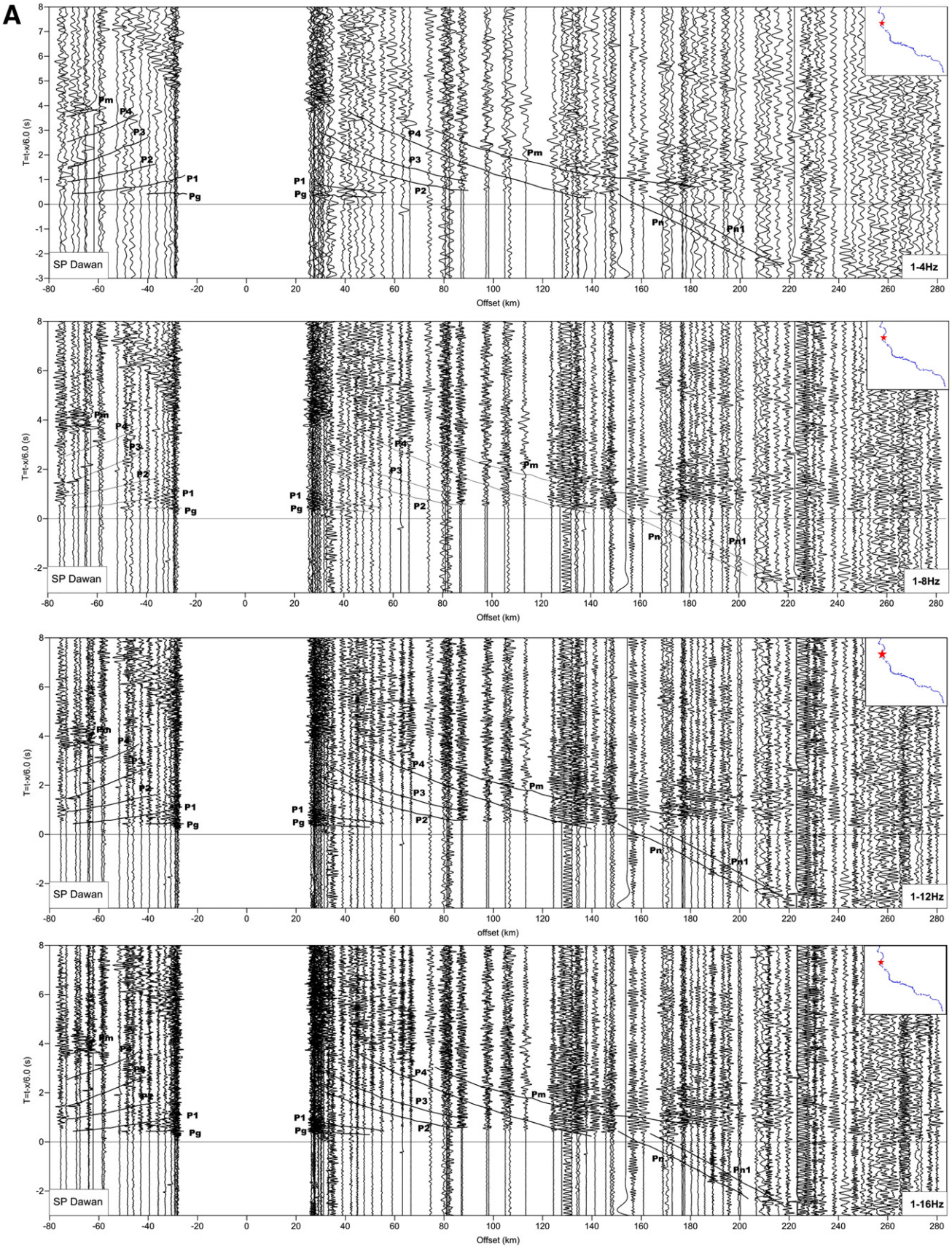

Fig. 3. P-wave vertical-component gathers from two inline shots fired at Dawan and Gangkou Island, following successive filtering by band-pass filters with frequency ranges of 1–4, 1–8, 1–12 and 1–16 Hz (from top to bottom). The inset at the upper right indicates the location of the shot point (star) on the seismic profile. All sections are shown at a reduced time scale using a reduction velocity of 6.0 km/s. The theoretical travel times computed from the crustal velocity model (Fig. 4) are depicted by continuous lines. Pg energy arrivals refracted above the crystalline basement, and PmP-waves reflected from the Moho and Pn-waves critically refracted from the Moho, may be identified easily. Other seismic phases reflected from interfaces between the crystalline basement and the crust–mantle discontinuity, labeled P1 to P4, may be recognized with different amplitudes.

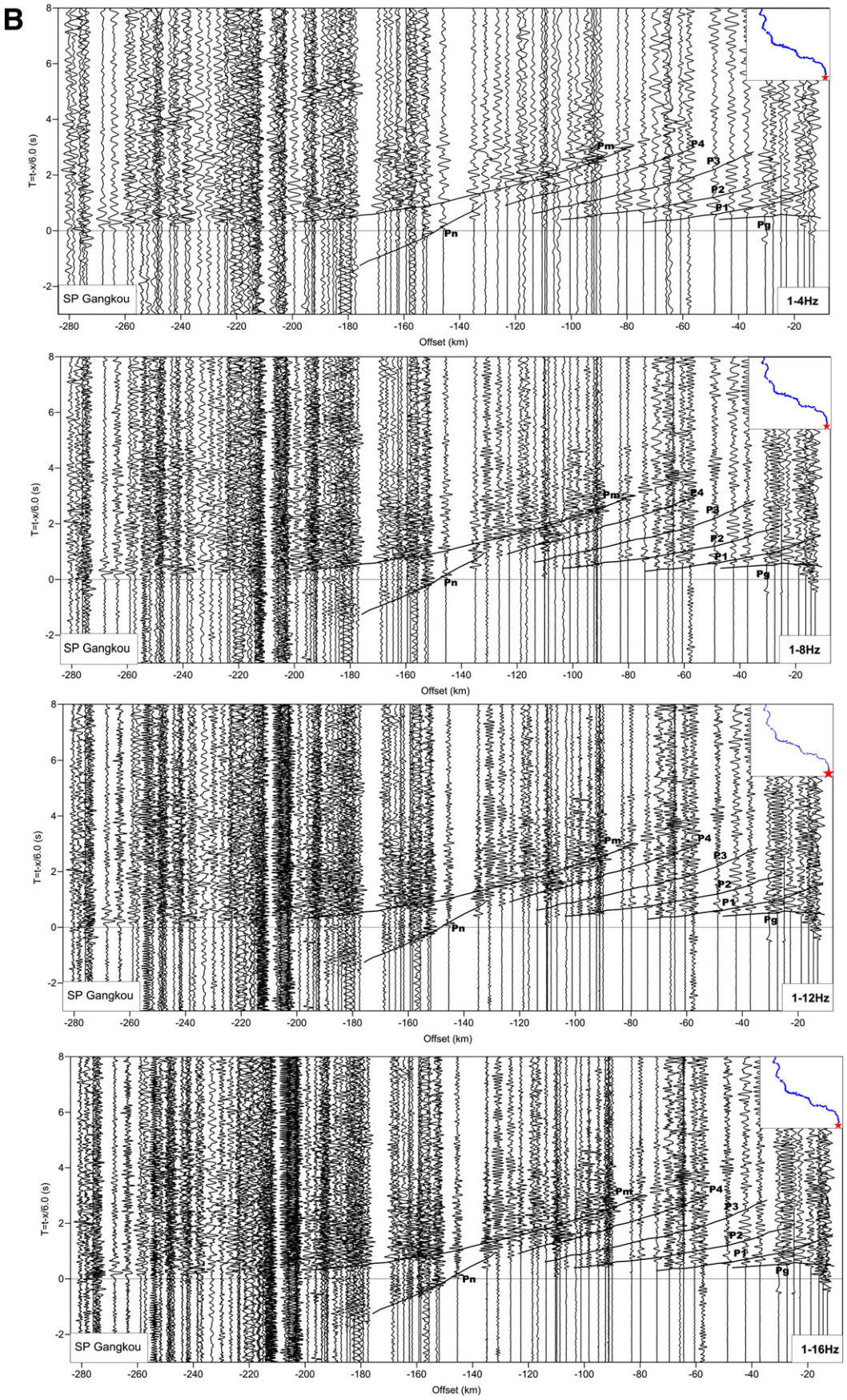

Fig.3 (*continued*).

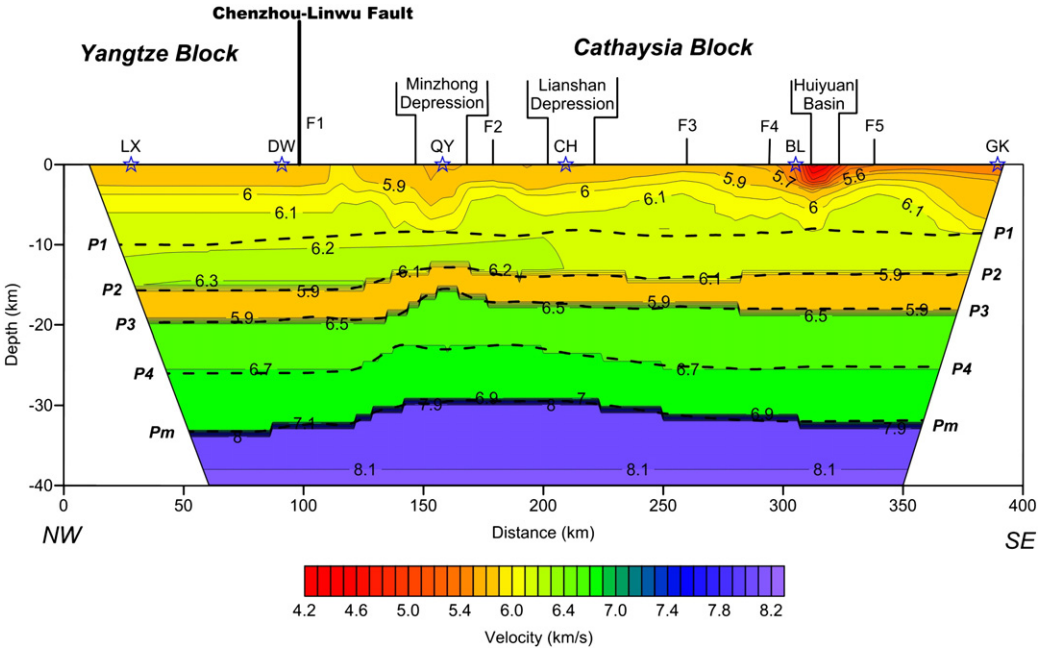

Fig. 4. P-wave velocity model for the Lianxian–Gangkou transect (velocities are given in km/s). The positions of the shot points fired during the experiment, Lianxian (LX), Dawan (DW), Qingyuan (QY), Conghua (CH), Boluo (BL) and Gangkou (GK), and also the positions of the major active faults (F1 to F5), depressions and basins are shown on surface where they are intersected by the profile. At increasing depths, those discontinuities that cause reflection events P1 to P4 and Pm are depicted by continuous lines. The different structures, upper, middle, and lower crust, the Moho discontinuity and the uppermost mantle, all delineated by velocity isolines, can clearly be seen.

5. Discussion

In order to determine the seismological response of the crust to the intraplate compression and extension, we adopt two approaches: in the first, we consider the crystalline basement and consolidated crust, and in the second, we focus on the spectral contents of the multi-filtered reflection sections obtained from common shot gathers and observe the seismic responses of the deep crustal formations to the northwest and southeast of the CLF.

As the objective of this study, we will aim to relate lithosphere evolution beneath the Cathaysia and the Yangtze blocks to systematic seismic variations within the crust, such as: (1) the asymmetry between tectonic blocks to show the aging difference of consolidated crust between the Cathaysia and the Yangtze blocks; (2) distinctive lateral variations of average seismic velocity and the corresponding thickness both of sediment layer and consolidated crust; (3) coastward increasing of seismic reflection strength within Cathaysia.

5.1. Systematic variations in seismic velocity and reflections within the crust

5.1.1. Lateral variation of average P wave velocity and thickness in the sedimentary and consolidated crustal layers

The lateral variation of block age imprints tectonic activity between different tectonic blocks. It is a common approach to use seismic velocity to infer aging of sedimentary basins (Wyllie et al., 1956) in qualitative and quantitative geological interpretation. Geological studies show that the age of the crystalline basement beneath the Cathaysia block is about 2.5 Ga (Chen and Jahn, 1998; Wang et al., 2003). The Yangtze block is significantly older at 2.7–2.8 Ga, or even 3.2 Ga (Shui, 1988; Ren et al., 1990; Qiu et al., 2000). This lateral variation in the age of crystalline basement can be evaluated with seismic P-wave velocity distribution, which is seismic responses to the accretion of Cathaysia onto the Yangtze Block (Su et al., 2009; Wong et al., 2011).

Taking into account the uncertainty in the P-wave velocity model (Fig. 4), we now attempt to characterize this structure using trial values of velocity of 5.8, 5.9, 6.0 and 6.1 km/s, and then estimate the sediment thickness (Fig. 6a) and the average P-wave speed (Fig. 7a). We observe in Fig. 6a that the crystalline basement depth remains fairly constant to the northwest of the CLF (Yangtze block), while it changes abruptly to the southeast of the CLF (Cathaysia block), giving rise to remarkable fluctuations when the sediment layer meets the tilted orientation of the CLF. In Fig. 7a we see that the P-wave speed beneath the Cathaysia block is generally lower than it is beneath the Yangtze block. Although we cannot calculate the age of the basement directly, we can nevertheless make an estimate of it because both the thickness and the P-wave velocity of the sedimentary layer depend on its age with assumption of compaction of porous media (Wyllie et al., 1956). The youngest sedimentary rocks are Paleozoic in age, and so all rocks are probably fully compacted by now. P-wave velocities show a strong relationship with the maximum depth of burial (either preserved in basin depth, or as metamorphic grade at the surface). So it is expected that P-wave velocity-"depth" relationship, over the "age" relationship (as the oldest rocks are probably the deepest buried) exists. Using this criterion, we can indirectly infer whether a tectonic formation is geologically older or younger than an adjacent block. In our case, the thickness and average P-wave velocity affecting the sedimentary rocks beneath each of the two blocks in question (Figs. 6a and 7a) suggest that the Cathaysia block is younger than the Yangtze block, which is consistent with their respective ages as determined by other methods.

The foregoing results allow us to calculate the crustal thickness, here understood to be seen in the dataset between the base of the sediments and the Moho (Fig. 6b), as well as the average P-wave velocity of the crystalline crust (Fig. 7b). As before, we observe in Fig. 6b that the thickness of the crystalline crust remains fairly constant to the northwest of the CLF (Yangtze block), while it changes abruptly and decreases to the southeast of the CLF (Cathaysia block). Analogously, in Fig. 7b we see that the P-wave velocity beneath the Cathaysia block is generally lower than it is beneath the Yangtze

block. These systematic lateral variations in thickness and P-wave velocity of the sedimentary layer and the crystalline crust are interpreted to represent the response of the crustal involvement in the deformation from intraplate orogeny and postorogenic magmatism.

5.1.2. Lateral variation of amplitude–frequency curves in the sedimentary and consolidated crustal layers

The shot fired at Dawan provides a unique opportunity to assess the differences between the two blocks because the site is located just on

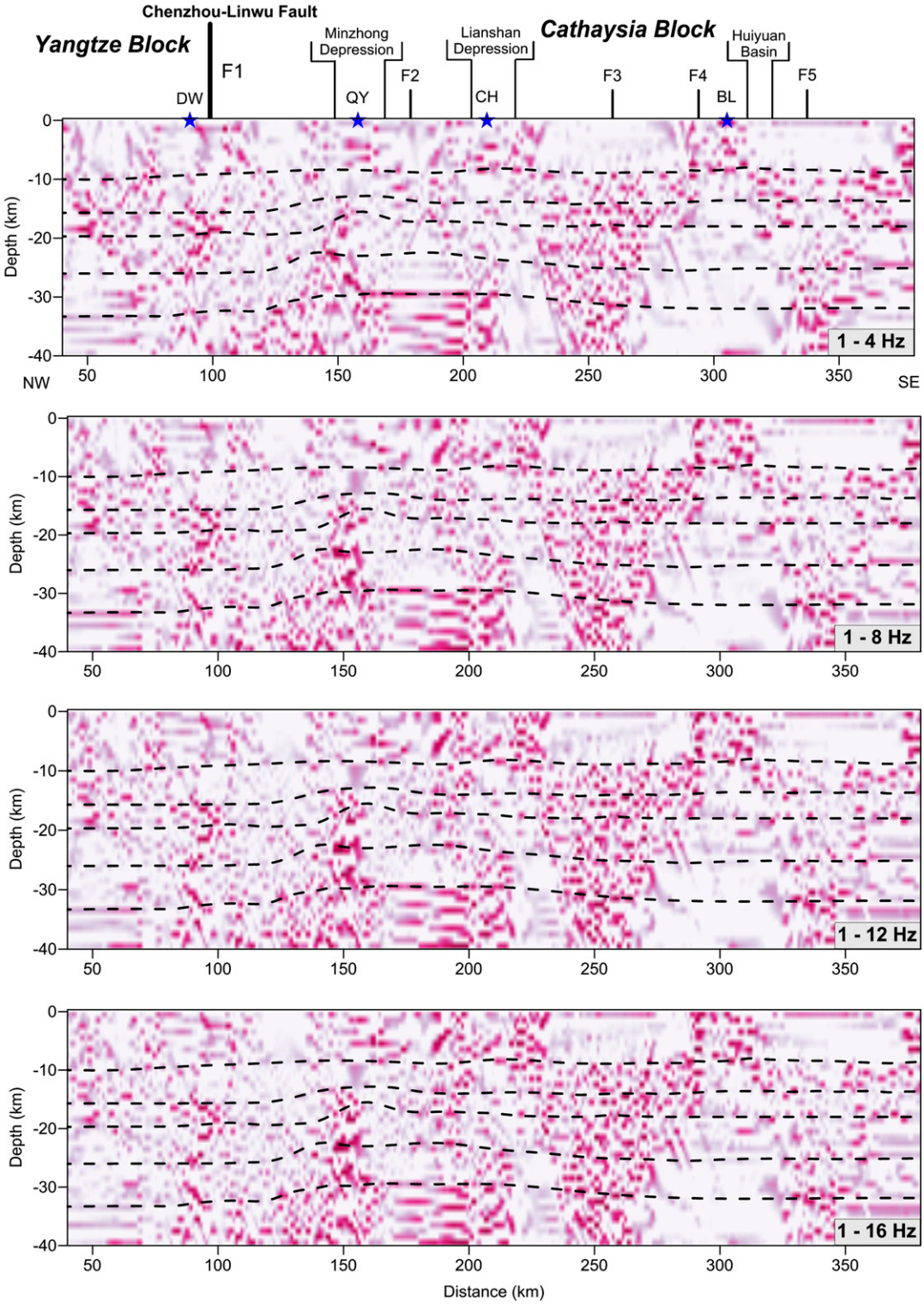

Fig. 5. Reflection structures of the crust and uppermost mantle along the Lianxian–Gangkou transect, obtained from pre-stack migration of wide-angle seismic data filtered within the frequency ranges 1–4, 1–8, 1–12 and 1–16 Hz. As before, the positions of the shot points fired during the experiment, Lianxian (LX), Dawan (DW), Qingyuan (QY), Conghua (CH), Boluo (BL) and Gangkou (GK), and also the positions of the major active faults (F1 to F5), depressions and basins, are shown on the surface where they intersect the profile. P1, P3 and PmP show the seismic events seen in Fig. 3.

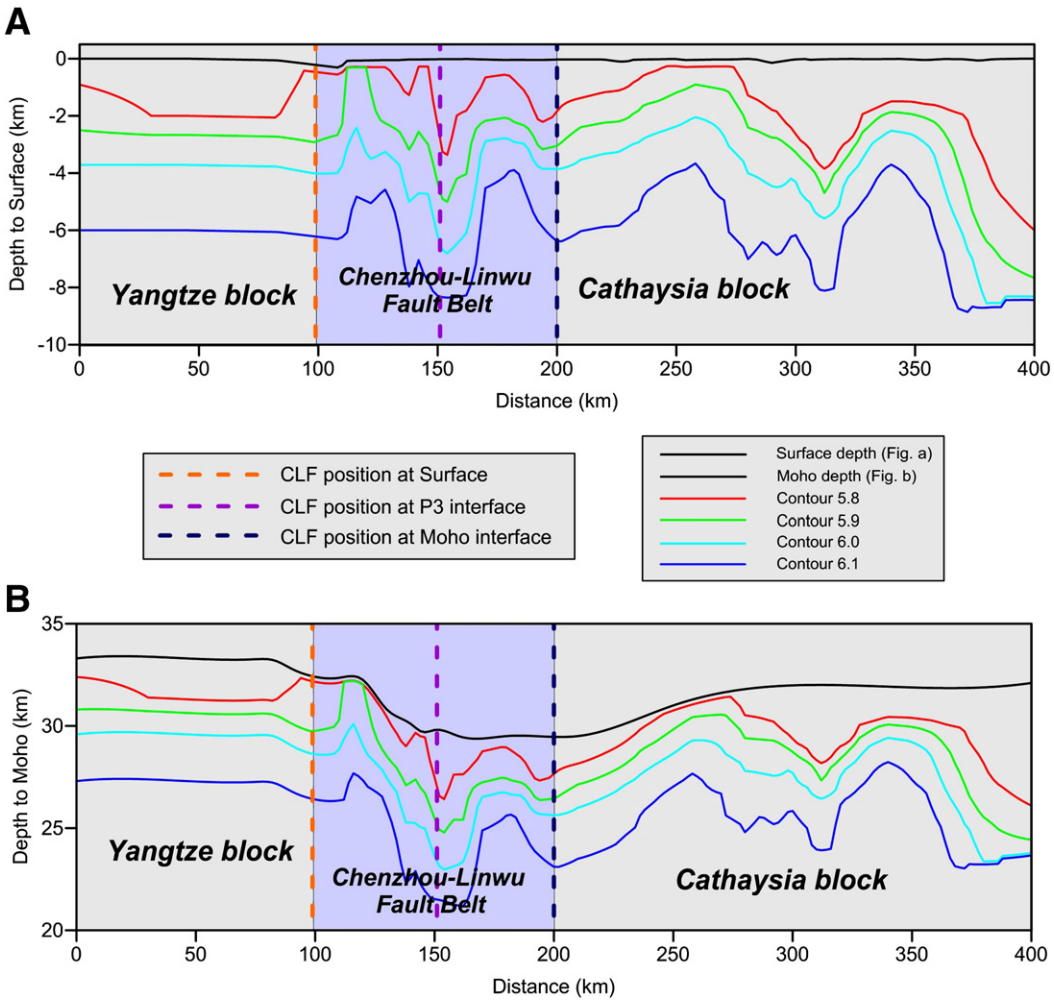

Fig. 6. Laterally varying thickness of the sediment layer (a) and variable depth of the consolidated crust (b) along the Lianxian–Gangkou seismic profile. The vertical dashed lines at different offsets refer to the position to which the CLF in its progressive penetration meets the interfaces indicated in the inset.

the CLF, and its branches lie on opposite sides to the northwest and southeast of the fault (Fig. 1), i.e., on the Yangtze and the Cathaysia blocks, respectively. We used the crustal P-wave velocity model (Fig. 4) to determine the time windows for the two types of seismic events transmitted beneath the Yangtze and Cathaysia blocks, which include well-developed crustal reflections from the bottom of the upper crust and the Moho. In the lower part of the first of these figures, several beams of reflected rays are shown passing through the Yangtze and Cathaysia blocks, which represent P1 and PmP events generated at Dawan. In the upper part we have a variety of amplitude–frequency curves for these events P1 (top) and PmP (bottom), after applying the band-pass filters of 1–4, 1–8, 1–12, and 1–16 Hz. In the case of the P1 reflections from the bottom of the upper crust beneath the Yangtze block, the dominant frequency is about 6 Hz, becoming 8 Hz beneath the Cathaysia block. For the PmP phase, the dominant frequency tends to increase progressively in Yangtze, while it remains constant at about 6 Hz in Cathaysia.

In the same way, in the lower part of the second of these figures, two beams of reflected rays are shown passing through the Cathaysia block, which represent P1 and Pm events generated at Gangkou (Fig. 9), and in the upper part we show various amplitude–frequency curves for these events. The same picture persists in terms of P1 and PmP events beneath the Cathaysia block, because their corresponding spectra, in particular for PmP, have similar shapes (Figs. 8 and 9). For the PmP phase the dominant frequency is therefore about 6 Hz. These differences in seismic frequency can be interpreted in the context of intraplate compression and its successive extension in South China. Similar structure pattern was observed as surface geological evidence of inversion tectonics in the pre-Andean basement of the Sierra de Cachi, Salta, Argentina (Tubía et al., 2012).

This lateral variation of amplitudes of the P3 and PmP phases (Fig. 10) can be further confirmed by the wide-angle prestack migration sections (Fig. 5). These amplitudes are determined using time-variable spectral analysis applied to the wide-angle seismic signals (Fig. 5) within the frequency intervals of interest. At a distance of 150 km from the origin of the profile, the change in amplitude of the seismic reflections may be seen from the bottom of the middle crust (P3) when passing from one side of the CLF to the other, suggesting that this fault really does reach the bottom of the middle crust, and does so with a slope of some 22°. A similar change in amplitude between the two sides of the CLF may be seen even more clearly at 200 km (Fig. 10), where the slope of the fault as it crosses the lower crust is very similar. The same conditions apply in the case of seismic reflections from the Moho, such that the fault continues down as far as the deep crust.

5.2. Characterization of the contact between the Yangtze and Cathaysia blocks

The CLF (or WSF) is inferred to be the contact boundary between the Yangtze and Cathaysia blocks, as suggested by the crustal velocity model (Fig. 4), surface geological mapping (Zhang et al., 1984; Angelier, 1990; Hou and Li, 1993) and the ages of rock samples (Li and Li, 2007). Our above-mentioned systematic variations of average P-wave velocity and

thickness both of the sedimentary and consolidated crustal layers support the inference that the CLF is also interpreted to be a crustal scale fault (Wang et al., 2003; Li and Li, 2007; Zhang and Wang, 2007), but the geometry of the CLF is still unclear. The geometry of the CLF is important to constrain the crustal contact relationship between the two tectonic blocks, i.e. whether it is vertical block to block contact or low-angle faulting between the two tectonic blocks.

To this end, we focus on the spatial variation of the deep crust along the LG profile, by combining the amplitudes of the P3 and PmP phases (Fig. 10). These amplitudes are determined using time-variable spectral analysis applied to the wide-angle seismic signals (Fig. 5) within the frequency intervals of interest. At a distance of 150 km from the origin of the profile, the change in amplitude of the seismic reflections may be seen from the bottom of the middle crust (P3) when passing from one side of the CLF to the other, suggesting that this fault really does reach the bottom of the middle crust, and does so with a slope of some 22°. A similar change in amplitude between the two sides of the CLF may be seen even more clearly at 200 km (Fig. 10), where the slope of the fault as it crosses the lower crust is very similar. The same conditions apply in the case of seismic reflections from the Moho, such that the fault continues down as far as the deep crust.

The geometry of the CLF may be explained by a greater dip angle where it penetrates the brittle upper crust, which becomes slightly smaller when the fault sinks in the middle and lower crust as it is affected by the regional tectonics. Such a characteristic may also be observed in other environments and extensional areas, as demonstrated by near-vertical seismic reflection experiments (Bally et al., 1966). The geometry of the CLF is consistent with the crustal rheology of South China as supported by the occurrence of earthquakes in the region, which are certainly constrained to the brittle upper crust (Zhang et al., 2011a). The geometry of the CLF and the strong deformation revealed by the P-wave velocity and thickness of the crust (Figs. 4 and 5) may indicate lithospheric extension (or rollback) towards the coast following the intraplate orogeny. The increase in strength of the wide-angle seismic reflections from the bottom of the upper crust and the Moho discontinuity suggest Mesozoic coherent deformation and an increase in Mesozoic magmatism towards the coast.

5.3. Possible mechanisms to explain the systematical seismic variations within the crust beneath the Cathaysia block

The tectonic evolution of the South China block remains a matter of some dispute. However, the seismic structure of the deep crust provides tighter constraints on the evolution of the regional tectonics. Proposed models include an Andean-type active continental margin (Guo et al., 1983), an Alpine-type collision belt (Hsü et al., 1988, 1990; Wang and Liu, 1992), and lithospheric subduction (Holloway, 1982; Faure, 1996; Zhou and Li, 2000) with an underplating of mafic magma (Li and Li, 2007). In order to understand the possible mechanism to explain the systematical seismic variations within the crust beneath the Cathaysia block, we construct a >1000-km-long transect (lower panel, Fig. 11) by taking advantage of the numerous deep seismic soundings and

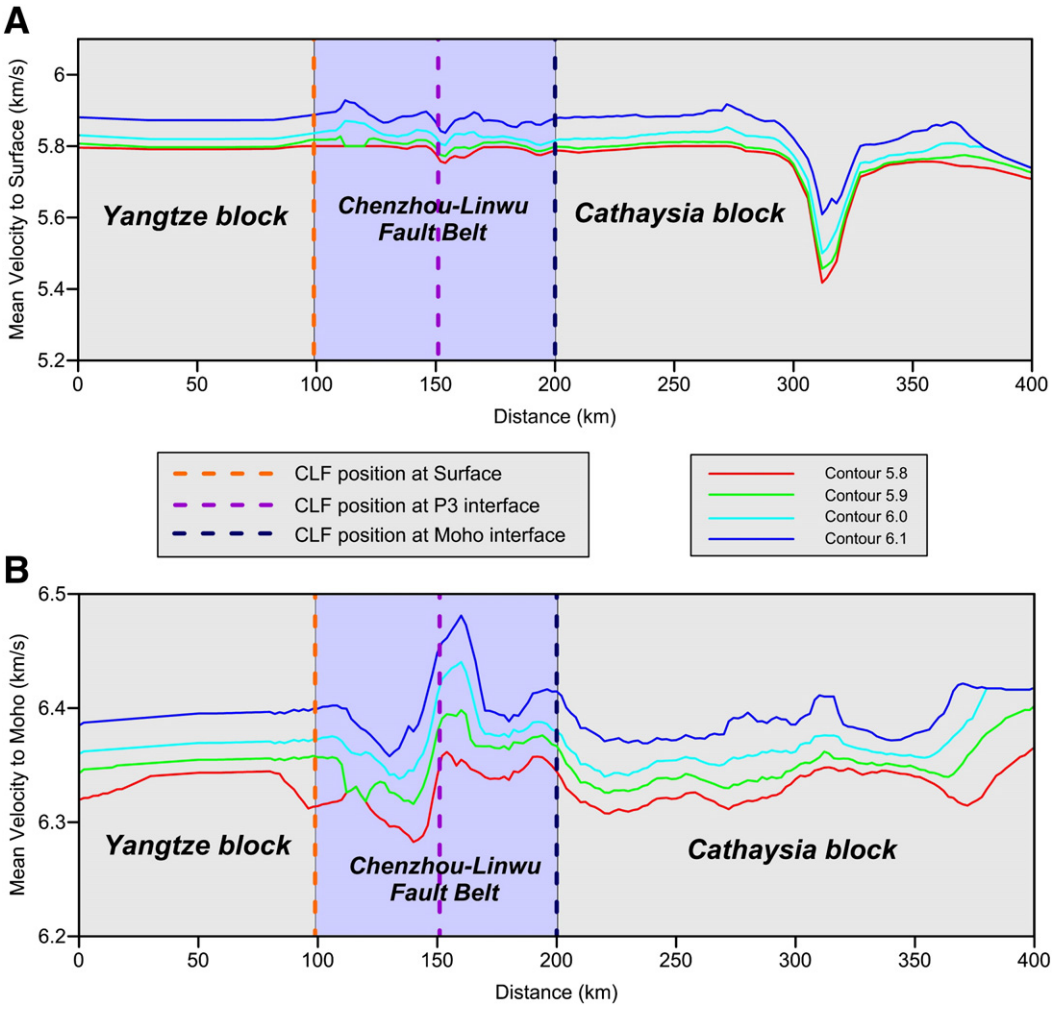

Fig. 7. Average P-wave velocity of the sedimentary layer (a) and the consolidated crust (b) along the Lianxian–Gangkou seismic profile. The vertical dashed lines at different offsets refer to the position to which the CLF in its progressive penetration meets the interfaces indicated in the inset.

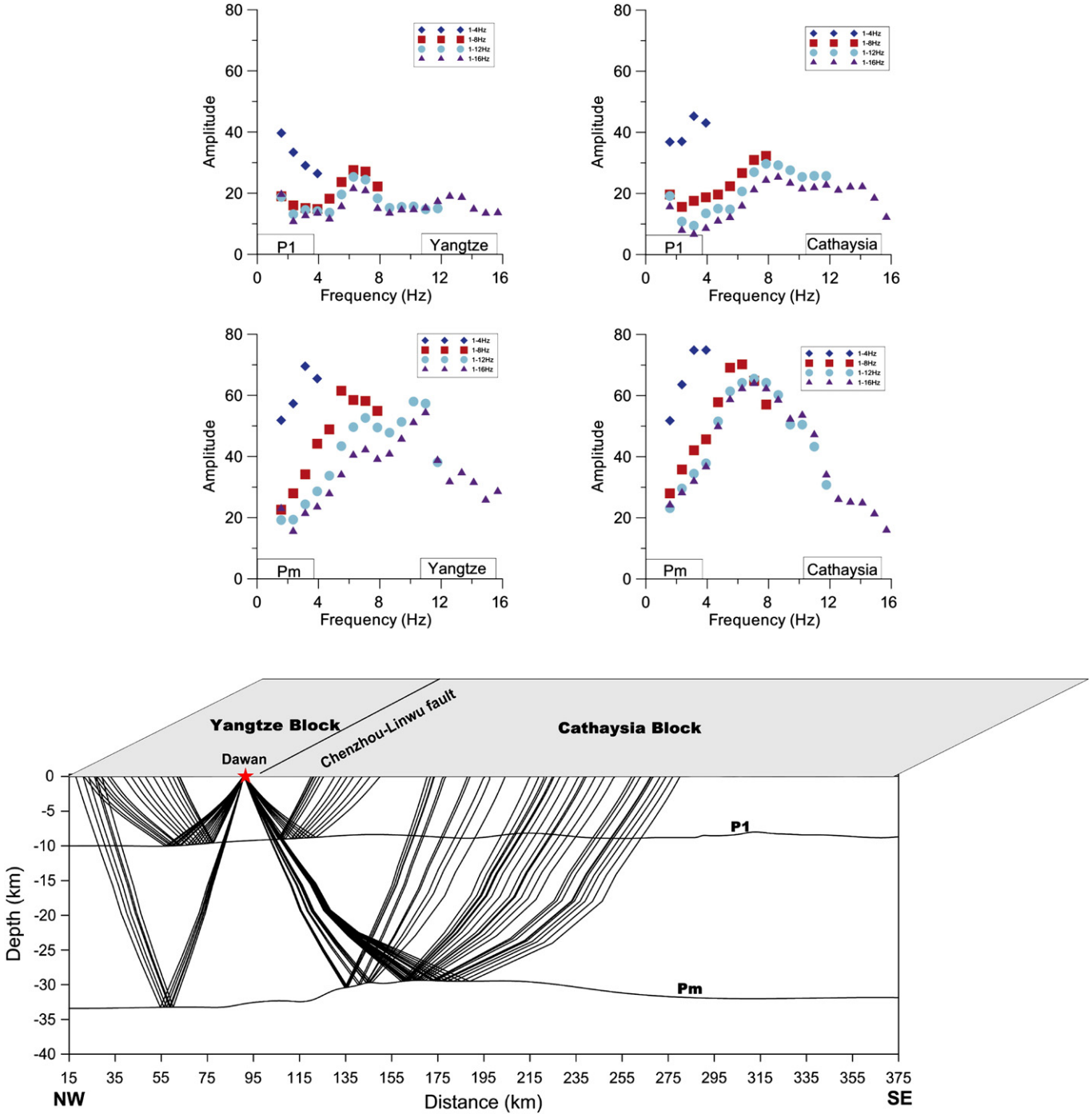

Fig. 8. Amplitude spectra obtained from multi-filtered reflection events P1 and PmP generated at Dawan, which give rise to several beams of reflected rays going through the Yangtze and Cathaysia blocks (lower part). The illustration shows the variety of amplitude–frequency curves beneath the Yangtze (left) and the Cathaysia (right) blocks for events P1 (top part) and PmP (central part) after applying band-pass filters of 1–4, 1–8, 1–12 and 1–16 Hz.

near-vertical seismic reflection experiments performed during the last 30 years (Yuan et al., 1989; Wei et al., 1990; Nissen et al., 1995a,b; Yin et al., 1999; Yan et al., 2002; Zhang and Wang, 2007; Zhang et al., 2009a,b; Yao et al., 2011). Where, data on lithospheric thickness were collected from surface wave tomography (Zhu et al., 2002).

Clearly, P-wave velocity distribution in the crust (Fig. 4) displays an intermediate lower crust featured with P-wave velocity of about 6.8 km/s in the lower crust (Christensen and Mooney, 1995; Li et al., 2006; Zhang et al., 2008, 2011a, 2011b), which is not compatible with mafic or even ultramafic lower crust with P-wave velocity of >7.0 km/s required by underplating (Thybo et al., 2000, 2009; Zhang et al., 2009a, 2009b, 2011a, 2011b). Thus underplating in reference to the tectonic evolution of the South China continent (Li and Li, 2007) can be excluded. We were not able to extract any evidence in support of the closure model of an oceanic basin in the South China block (Holloway, 1982; Hsü et al., 1990; Faure, 1996; Zhou and Li, 2000) because no relatively smaller-scale anomaly with high-velocity body could be detected in the wide-angle seismic data (with the limited lateral resolution). It is worth noting that one higher P-wave velocity layer (about 7.2 km/s) at the bottom of the lower crust, can be observed in the 1300-km-long transect (lower

panel, Fig. 11), and such features are usually considered to be a seismic signature of underplating (Christensen and Mooney, 1995; Thybo et al., 2000; Thybo and Nielsen, 2009; Zhang et al., 2009a, 2009b, 2010; Deng et al., 2011).

The significant changes observed in the intracrustal reflections at the offsets from 100 to 200 km of the LG profile (Fig. 5), and the findings on the geometry of the CLF (Fig. 10, lower panel, Fig. 11), which correspond to the contact belt between Yangtze and Cathaysia, are not in conflict with the postulated wrench faulting (Xu et al., 1993), or continental rifting and lithospheric extension models (Gilder et al., 1996; Li et al., 2000; Wang et al., 2003). These models may be considered in the light of the lateral variation of the crust along the LG profile, especially to the southeast of the CLF, and the topography of the Moho with small undulation at an offset of 140–240 km (Fig. 4). This geodynamic scenario well may be the result of the thrusting of the Pacific plate beneath the South China continent, or could be caused by the underthrusting of the Yangtze Block beneath the Cathaysia Block along the boundary during the Mesozoic or Cenozoic (Rowley et al., 1989; Wang et al., 2010, 2011). All the proposed models of evolution suggest a predominantly compressive regime in South China and that intraplate lithospheric extension and thinning have dominated since the Early Mesozoic (Li et al., 1989; Faure,

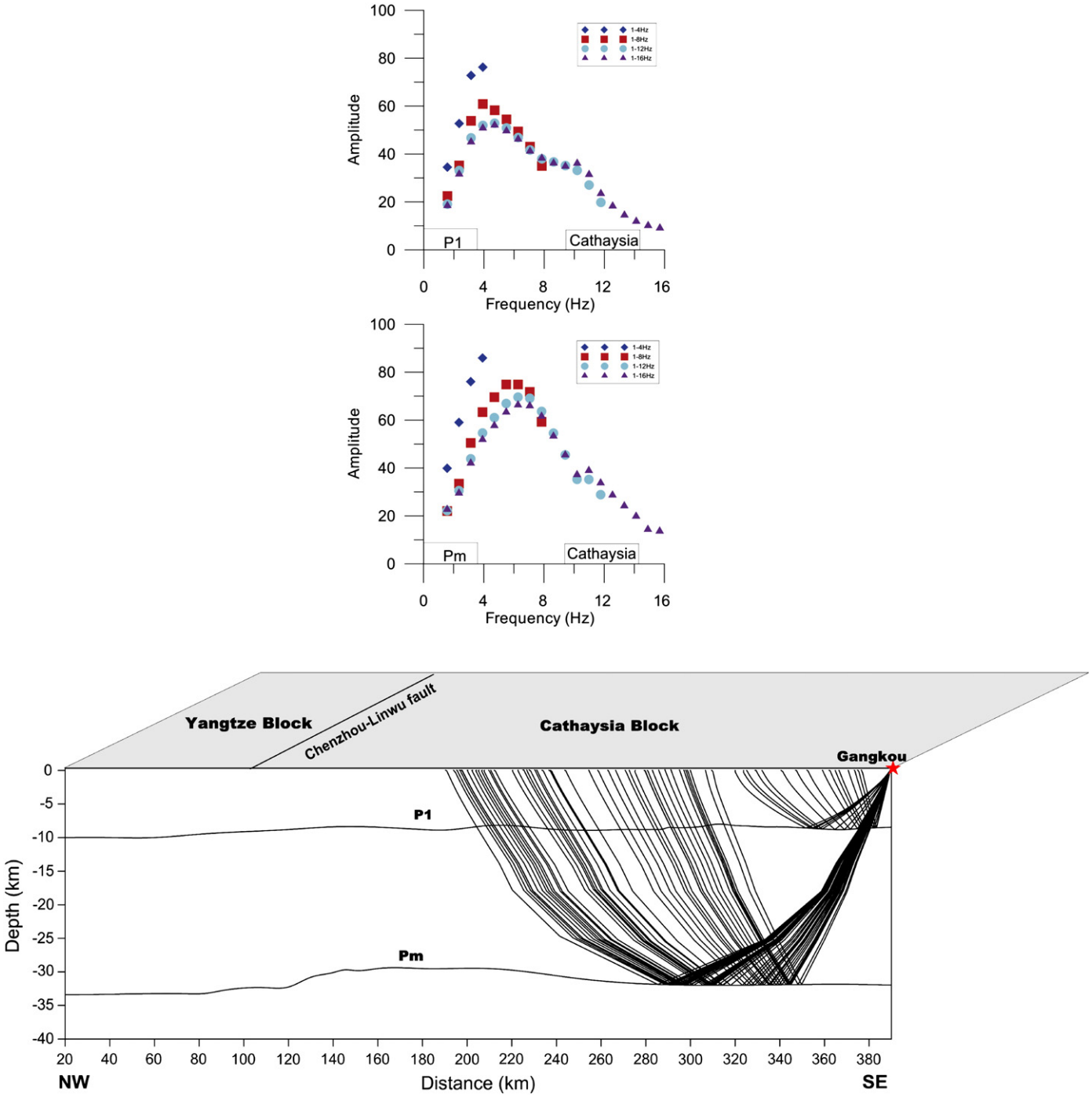

Fig. 9. Amplitude spectra obtained from multi-filtered reflection events P1 and PmP generated at Gangkou, which give rise to two beams of reflected rays that pass through the Cathaysia block (lower part). The illustration shows the variety of amplitude–frequency curves for events P1 (top part) and Pm (the central part) after applying band-pass filters 1–4, 1–8, 1–12 and 1–16 Hz.

1996; Gilder et al., 1996; Li et al., 2000; Wang et al., 2003; Li and Li, 2007; Chen et al., 2011). Beneath the southeastern segment of the LG profile and in a seaward direction, there is an increase in the amplitude of the wide-angle seismic reflections from the bottom of the middle crust and the Moho discontinuity for all the seismic frequency bands of interest (Fig. 5).

Mesozoic Lithospheric extension beneath the Cathaysia is widely accepted, but without agreement in its mechanism. Usually, there are at least three sorts of models to explain lithospheric extension, such as simple shear (Wernicke, 1985), pure shear (McKenzie, 1978; Ruppel, 1995), and magma compensated crustal extension models (Thybo and Nielsen, 2009). Our observation of lateral variations in velocity and thickness for the sedimentary and the consolidated crustal layers can be also taken as a seismic signature of the transition from intraplate compression at the CFL belt to extension beneath Cathaysia. Where, the CLF belt endured multiple episodes with earlier intraplate compression and later reactivation of extension. A simple-shear extensional regime (Wernicke, 1985) would be expected as the lithospheric structure as we have imaged in Fig. 11 looks remarkably like classic models. In a simple shear model, there is some uplift of Moho, which can be observed to a distance of 200 km in our 1300-km-long transect (lower panel, Fig. 11), but this model is unable to explain the strong reflective zone in the lower crust without abnormally high seismic velocity. Alternatively, the extension mechanism of magma compensated crustal thinning proposed in the Baikal rift zone (Thybo and Nielsen, 2009) can make a good explanation of the geometry of the CFL (fault flattening from a steep dip to a gentler way in the deep) and the relatively flat Moho (even though we can observe 1–2 km Moho undulation beneath the CLF), but not the intermediate lower crust in our observation. A pure shear model (McKenzie, 1978; Ruppel, 1995) can explain the uplift of the Moho in our observation (Fig. 11), but not the observation of intermediate composition with <7.0 km/s P-wave velocity lower crust.

This line of argument allows us to assess the intraplate extension as revealed by geochemical studies in South China (Wang et al., 2003). According to these studies, mafic rocks to the west of the Chenzhou-Linwu fault present EMI-like isotopic affinity enhanced by a relatively low Sr^{87}:Sr^{86} ratio, LREE enrichment and high LILE:HFSE ratio. In contrast, the mafic rocks to the east of the fault show a prevalent EMII-like isotopic signature with a significantly high Sr^{87}:Sr^{86} ratio and a relatively low LILE:HFSE ratio (Wang et al., 2003). This indicates that the Mesozoic mafic rocks near the Chenzhou-Linwu–Wuchuan-Sihui fault have different affinities for the enriched lithospheric mantle, and different tectonic histories. The spatial variation of the EMI–EMII-like signatures (lower panel, Fig. 11) related to the Mesozoic mafic rocks near the Chenzhou-Linwu–Wuchuan-Sihui fault, the thrust and the westward Early Mesozoic fold, together with important multi-metal mineralization, are all factors that support postorogenic magmatism (Gilder et al., 1996; Wang et al., 2003). From a seismological viewpoint, the listric geometry (vertically dip gentling) of the CLF indicates lithospheric extension, and the seismic velocity distribution in the crust and the outputs for different frequency bands provide clues for understanding the intraplate extension of the study area, and the increasing eruption of young

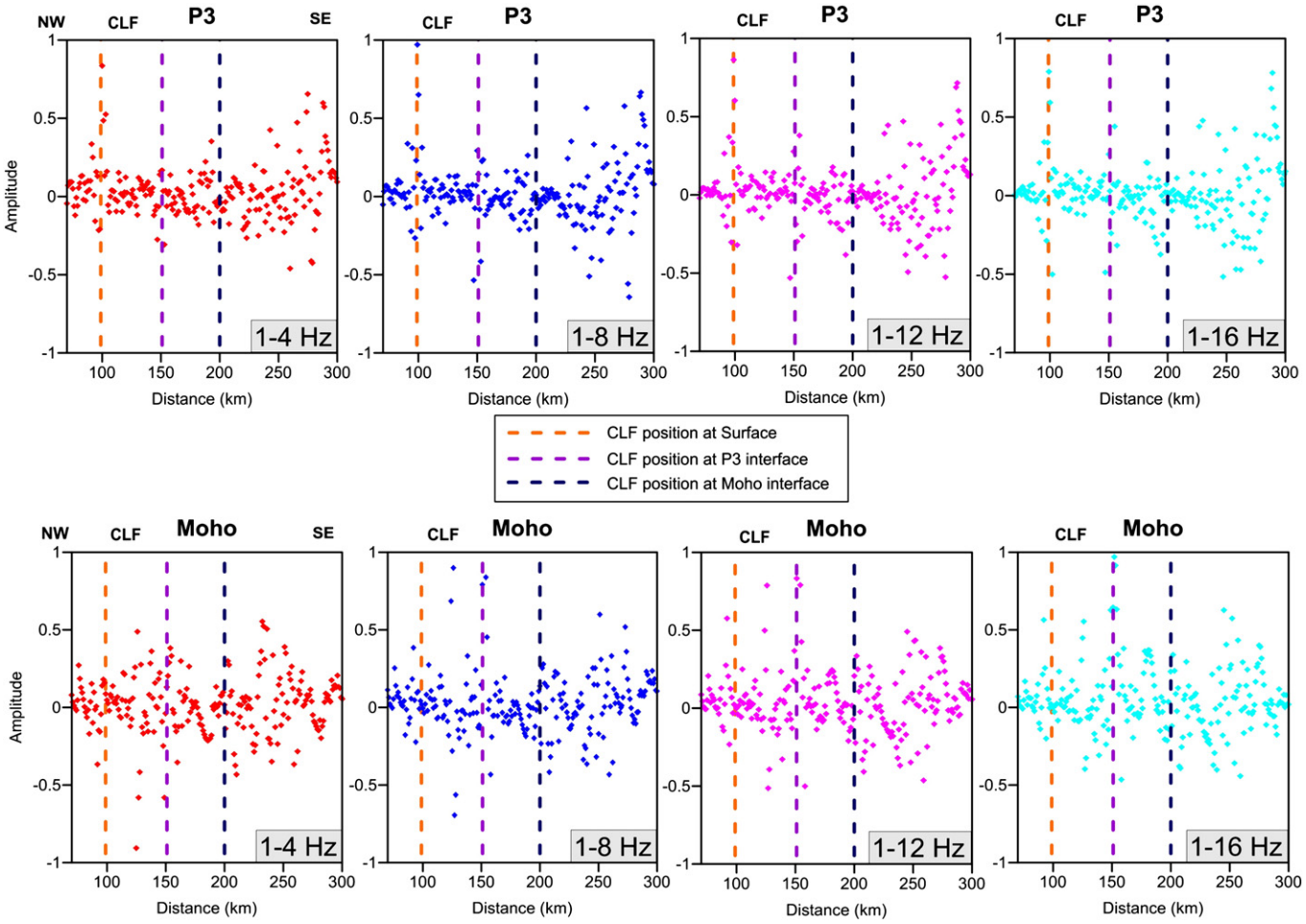

Fig. 10. Variation in amplitude of seismic events reflected on a deep interface below the crystalline basement (upper plots) and from the Moho (lower plots), determined through time-variable spectral analysis applied to the wide-angle seismic signals in Fig. 5 within the frequency intervals of interest. Vertical dashed lines at different offsets refer to the position to which the CLF in its progressive penetration meets the interfaces indicated in the inset.

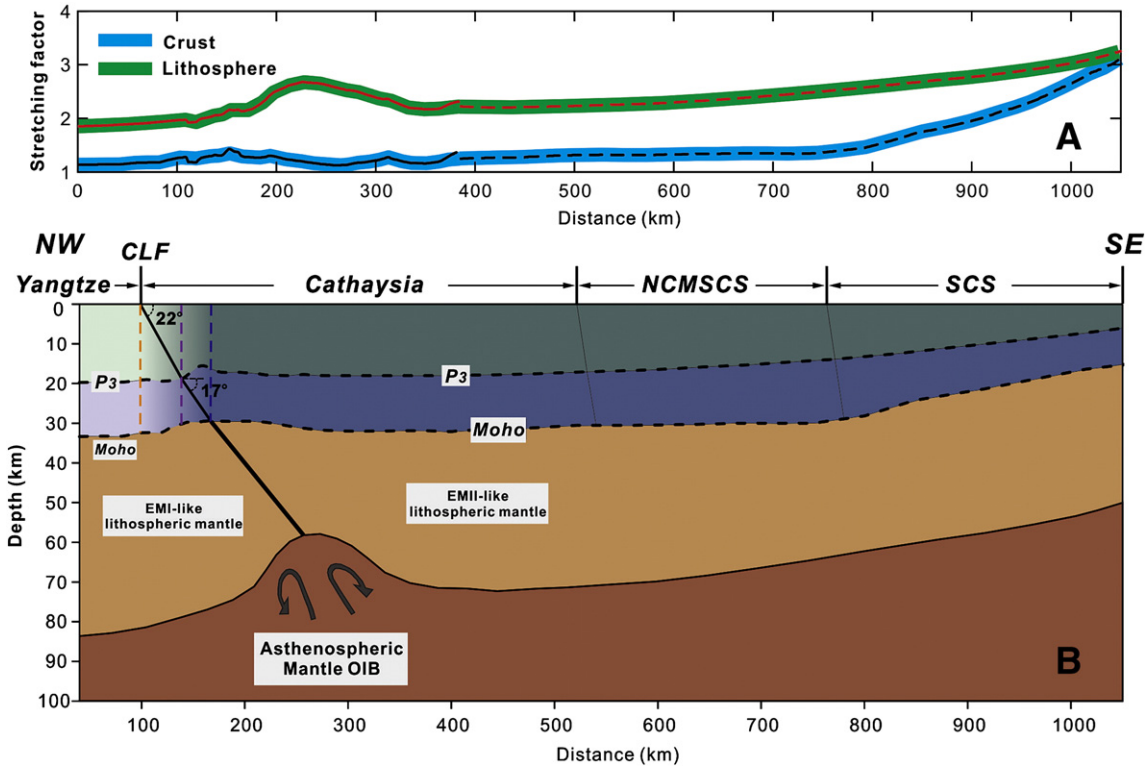

Fig. 11. Upper panel: extensional factors of whole crust and lithosphere beneath LG profile (in this study) and the northern margin of South China Sea (Zhang et al., 2010); lower panel: overview of the intraplate orogeny and postorogenic magmatism in South China. YB — Yangtze block; CB — Cathaysia block; NCMSCS — the northern continental margin of South China Sea; SCS — South China Sea; CLF — Chenzhou-Linwu Fault.

volcanic rocks to the east. The differences in the crustal velocity and reflection patterns shed some light on aspects of the tectonics or even the crustal composition related to the intraplate extension. Taking the typical P-velocity of 6.0 km/s as a means of delineating the crystalline basement, it may be seen that the thickness of sediments above the basement remains almost constant at around 4 km to the northwest of the CLF (Fig. 4); it is only when crossing the fault in a southeasterly direction that the sediment thickness clearly increases. This thickening of the sediment layer towards the coast may be interpreted to be the result of an increase in the eruption of volcanic rocks (Zeng et al., 1997; Zhou and Li, 2000; Teng et al., 2001a,b; Xiong et al., 2002; Wang et al., 2003; Yan et al., 2004; Zhao et al., accepted for publication, in preparation). The decrease in the vertical velocity gradient in the Cathaysia block is probably caused by the presence of these rocks that outcrop so abundantly, as revealed by surface geological mapping (Fig. 1).

We calculate the extensional factors with the formula: pre-rift thickness/stretched thickness, for the crust and the lithosphere, respectively. By taking 35 km as the pre-stretch thickness of the crust (Nissen et al., 1995a, 1995b) and 150 km as the pre-stretch thickness of lithosphere in the South China (Zhu et al., 2002; Menzies et al., 2007; Zhang et al., 2012), The extensional factor (β) is estimated to be about 1.5 for the whole crust, and about 2.0 for the lithosphere along our LG profile (upper panel, Fig. 11). Incorporating the extensional factor (β) beneath the northern margin of the South China Sea estimated from deep seismic reflection sections that about 1.7–3.0 for the whole crust, and about 2.5–3.1 for the lithosphere beneath Cathaysia (Zhang et al., 2010), we can observe two kinds of features, namely (1) there is a discrepancy of extensional factor between the crustal- and the lithosphere-scale along the long transect and (2) the crustal-, lithosphere-scale extensional factors increase but their discrepancy decreases coastward (upper panel, Fig. 11). In addition to the discrepancy between the extensional factors at the crustal and lithospheric scale in the northern margin of the South China Sea (Zhang et al., 2010), and coastward decreasing of the discrepancy between the crustal- and the lithosphere-scale extensional factors (upper panel, Fig. 11), the eastwards strengthening of the seismic reflections beneath the Cathaysia block (Fig. 10) may be the seismic signature of the magma intrusion in the lower crust: either as a result of lithospheric extension due to the subduction of the western Pacific plate or mantle extrusion (Driscoll and Karner, 1998; Davis and Kusznir, 2004; Zhang et al., 2010, 2011b), which probably hint the more studies need to reconsider the origin of the opening of South China Sea.

6. Conclusions

Images of wide-angle seismic reflections in the crust along the northwest–southeast seismic profile between Lianxian and Gangkou, South China, have been obtained by applying the technique of depth-domain pre-stack migration to seismic signals pre-processed using different band-pass frequency filters. Although there are several events that have relatively high amplitudes, two depth levels seem to be the origins of higher amplitude reflections: these correspond to the bottom of the upper crust (~15 km depth) and the crust–mantle discontinuity (33–35 km depth). Our key findings can be summarized as follows: a) the thickness and average P-wave velocity both of the sedimentary layer and the crystalline basement are characterized by abrupt lateral variations towards the coast from the CLF, which suggests that the deformation is well developed throughout the whole crust there. b) The reflection amplitudes observed from the crust–mantle boundary are sufficiently strong to suggest that there is no significant partial melt in the lower crust. c) The reflection strength patterns make it clear that the CLF is the natural contact border between the two major tectonic blocks of Yangtze and Cathaysia. This fault penetrates with a dip angle of about 22° to the bottom of the middle crust, below which it sinks with a dip angle of less than 17° down to the Moho, suggesting a ductile thick layer beneath the South China continent. d) The combination of the crustal P-wave velocity structure, multi-filtered wide-angle seismic reflections and lithospheric thickness

across the South China continent causes the constraining of the wholesale crustal deformation beneath the Cathaysia. e) The deepening of the crystalline basement to the southeast of the CLF, the strong changes observed in the seismic reflection patterns and together with depth-dependent extension beneath the Cathaysia and the northern margin of South China continent are probably the response of the crust to the extensive intraplate extension and the existence of young volcanic activity caused by lithospheric extension resulting from the subduction of the western Pacific plate, or by mantle extrusion.

Acknowledgments

We are indebted to Professor Zhouxun Yin, Dr. Zhiming Bai, Dr. Lin Chen and others who oversaw the acquisition of the seismic data at the CAS Institute of Geophysics, and who helpfully supplied us with the necessary geophysical information. We also are grateful to Professors Jiwen Teng, Xiangru Kong, Yafen Yan, W. Jacoby and three anonymous referees for their constructive comments and suggestions. The study is achieved with special contributions from Professors A. Aitken and M. Santosh. This research project was supported by the National Nature Science Foundation of China (41021063, 41074033, 40830315, and 40874041), the Ministry of Science and Technology of China (Sinoprobe-02-02, 2008ZX05008-006), and the Chinese Academy of Sciences (KXCX2-109, KZCX2-YW-132).

References

Angelier, J., 1990. Inversion of field data in fault tectonics to obtain the regional stress. III. A new rapid direct inversion method by analytical means. Geophysical Journal International 103, 363–376.
Bally, A.W., Gordy, P.L., Stewart, G.A., 1966. Structure, seismic data, and orogenic evolution of southern Canadian Rocky Mountains. Bulletin of Canadian Petroleum Geology 14 (3), 337–381.
Charvet, J., Shu, L.S., Shi, Y.S., Guo, L.Z., Faure, M., 1996. The building of south China: collision of Yangzi and Cathaysia blocks, problems and tentative answers. Journal of Southeast Asian Earth Sciences 13, 223–235.
Chen, J.F., Jahn, B.M., 1998. Crustal evolution of south-eastern China: Nd and Sr isotopic evidence. Tectonophysics 284, 101–133.
Chen, C.H., Hsieh, P.S., Lee, C.Y., Zhou, H.W., 2011. Two episodes of the Indosinian thermal event on the South China Block: constraints from LA-ICPMS U–Pb zircon and electron microprobe monazite ages of the Darongshan S-type granitic suite. Gondwana Research 19 (4), 1008–1023.
Christensen, N.I., Mooney, W.D., 1995. Seismic velocity structure and composition of the continental crust: a global view. Journal of Geophysical Research 100, 9761–9788.
Davis, M., Kusznir, N., 2004. Depth-dependent lithospheric stretching at rifted continental margins. In: Karner, G.D. (Ed.), Proceedings of NSF Rifted Margins Theoretical Institute, pp. 92–136.
Deng, Y.F., Li, S.L., Fan, W.M., Liu, J., 2011. Crustal structure beneath South China revealed by deep seismic soundings and its dynamics implications. Chinese Journal of Geophysics 54 (10), 2560–2574 (in Chinese).
Driscoll, N.W., Karner, G.D., 1998. Lower crustal extension across the northern Carnarvon Basin, Australia; evidence for an eastward dipping detachment. Journal of Geophysical Research. B: Solid Earth and Planets 103 (3), 4975–4991.
Duan, L., Meng, Q.R., Zhang, C.L., Liu, X.M., 2011. Tracing the position of the South China block in Gondwana: U–Pb ages and Hf isotopes of Devonian detrital zircons. Gondwana Research 19 (1), 141–149.
Faure, M., 1996. Extensional tectonics within a subduction-type orogen: the case study of the Wugongshan dome (Jiangxi Province, south-eastern China). Tectonophysics 263, 77–106.
Gao, Y., Wu, J., Cai, J.A., Shi, Y.T., Lin, S., Bao, T., Li, Z.N., 2009. Shear-wave splitting in the southeast of Cathaysia block, South China. Journal of Seismology 13 (2), 265–275.
Gilder, S.A., Gill, J., Coe, R.S., 1996. Isotopic and Paleo-magnetic constraints on the Mesozoic tectonic evolution of south China. Journal of Geophysical Research 107 (B7), 16137–16154.
Grabau, A.W., 1924. Migration of geosynclines. Geology Society China Bulletin 3, 207–349.
Greentree, M.R., Li, Z.X., Li, X.H., Wu, H., 2006. Late Mesoproterozoic to earliest Neoproterozoic basin record of the Sibao orogenesis in western South China and relationship to the assembly of Rodinia. Precambrian Research 151, 79–100.
Guo, L.Z., Shi, Y.S., Ma, R.S., 1983. On the formation and evolution of the Mesozoic–Cenozoic active continental margin and island arc tectonics of the western Pacific Ocean. Acta Geologica Sinica 1, 11–21.
Holloway, N., 1982. North Palawan block, Philippines: its relation to the Asian mainland and role in evolution of South China Sea. AAPG American Association of Petroleum Geologists Bulletin 66, 1355–1383.
Hou, Q.L., Li, J.L., 1993. A preliminary study on the foreland fold and thrust belt, southwest Fujian. In: Li, J.L. (Ed.), Lithospheric Structure and Geological Evolution of Southeastern Continent. Metallurgical Publishing House, Beijing, p. 264.
Hsü, K.J., Sun, S., Li, J.L., Chen, H.H., Pen, H.P., Sengor, A.M.C., 1988. Mesozoic overthrust tectonics in south China. Geology 16, 418–421.
Hsü, K.J., Li, J.L., Chen, H.H., Wang, Q.C., Sun, S., Sengor, A.M.C., 1990. Tectonics of South China: key to understanding west Pacific geology. Tectonophysics 183, 9–39.
Huang, T.K. (Ed.), 1980. Tectonic Evolution of China: Explanatory Notes for 1:4,000,000 Tectonic Map of China. Sci. Publ. House, Beijing, p. 124.
Jahn, B.M., Martineau, F., Peucat, J.J., Cornichet, J., 1986. Geochronology of the Tananao Schist complex, Taiwan. Tectonophysics 125, 103–124.
Jahn, B.M., Zhou, X.H., Li, J.L., 1990. Formation and tectonic evolution of Southeastern China and Taiwan: isotopic and geochemical constraints. Tectonophysics 183, 145–160.
Lafond, C.F., Levander, A., 1995. Migration of wide-aperture onshore-offshore seismic data, central California: Seismic images of late stage subduction. Journal of Geophysical Research 100 (B11), 22231–22243.
Li, J.L. (Ed.), 1992. Study on the Texture and Evolution of the Oceanic and Continental Lithosphere in Southeastern China. Chinese Science and Technology Press, Beijing.
Li, Z.X., Li, X.H., 2007. Formation of the 1300-km-wide intraplate orogen and postorogenic magmatic province in Mesozoic South China: a flat-slab subduction model. Geology 35 (2), 179–182. http://dx.doi.org/10.1130/G23193A.
Li, X., McCulloch, M., 1996. Secular variation in the Nd isotopic composition of Neoproterozoic sediments from the southern margin of the Yangtze block: evidence for collision in southeast China. Precambrian Research 76, 67–76.
Li, J.L., Sun, S., Hsü, K.J., Chen, H.H., Peng, H.P., Wang, Q.C., 1989. New evidence about the evolution of the South Cathaysia Orogenic Belt. Science Geologica Sinica 3, 217–225.
Li, Z.X., Zhang, L., Powell, C.M., 1995. South China in Rodinia: part of the missing link between Australia–East Antarctica and Laurentia? Geology 23, 407–410.
Li, X., Sun, M., Wei, G.J., Liu, Y., Lee, C.Y., Malpas, J., 2000. Geochemical and Sm–Nd isotopic study of amphibolites in the Cathaysia Block, southeastern China: evidence for an extremely depleted mantle in the Paleoproterozoic. Precambrian Research 102, 251–262.
Li, X.H., Li, Z.X., Zhou, H., Liu, Y., Kinny, P.D., 2002a. U–Pb zircon geochronology, geochemistry and Nd isotopic study of Neoproterozoic bimodal volcanic rocks in the Kangdian Rift of South China; implications for the initial rifting of Rodinia. Precambrian Research 113, 135–154.
Li, Z.X., Li, X., Zhou, H., Kinny, P.D., 2002b. Grenvillian continental collision in South China: new SHRIMP U–Pb zircon results and implications for the configuration of Rodinia. Geology 30, 163–166.
Li, X.H., Li, Z.X., Ge, W.C., Zhou, H.W., Li, W.X., Liu, Y., Wingate, M.T.D., 2003. Neoproterozoic granitoids in South China: crustal melting above a mantle plume at ca 825 Ma? Precambrian Research 122, 45–83.
Li, X.H., Li, W.X., Li, Z.X., Wang, J., 2005. Formation of the South China Block: evidence from Sibaoan orogenic magmatism. In: Wingate, M.T.D., Pisarevsky, S.A. (Eds.), Supercontinent and Earth Evolution Symposium. Geol. Soc. Aus., Fremantle, p. 86 (Abst. 81).
Li, S.L., Mooney, W., Fan, J., 2006. Crustal structure of mainland China from deep seismic sounding data. Tectonophysics 420, 239–252.
Li, Z.X., Bogdanov, S.V., Collins, A.S., Davidson, A., De Waele, B., Ernst, R.E., Fitzsimons, I.C.W., Fuck, R.A., Gladkochub, D.P., Jacobs, J., Karlstrom, K.E., Lu, S., Natapov, L.M., Pease, V., Pisarevsky, S.A., Thrane, K., Vernikovsky, V., 2008. Assembly, configuration, and break-up history of Rodinia: a synthesis. Precambrian Research 160, 179–210.
Lin, G., Wang, Y.H., 2005. The P-wave velocity structure of the crust mantle transition zone in the continent of China. Journal of Geophysics and Engineering 2, 268–276.
Martin, H., Bonin, B., Capdevial, R., Jahn, B.M., Lameyre, J., Wang, Y., 1994. The Kuiqi peralkaline granitic complex (SE China): petrology and geochemistry. Journal of Petrology 35, 983–1015.
McKenzie, D., 1978. Some remarks on the development of sedimentary basins. Earth and Planetary Science Letters 40, 25–32.
Menzies, M.A., Xu, Y.G., Zhang, H.F., Fan, W.M., 2007. Integration of geology, geophysics and geochemistry: a key to understanding the North China Craton. Lithos 96, 1–21.
Milkereit, B., 1987. Migration of noisy crustal seismic data. Journal of Geophysical Research 92, 7916–7930.
Milkereit, B., Epili, D., Green, A.G., Mereu, R.F., Morel-À-L'Huissier, P., 1990. Migration of wide-angle seismic reflection data from the Grenville front in Lake Huron. Journal of Geophysical Research 95 (B7), 10,987–10,998.
Nissen, S., Hayes, D., Buhl, P., Diebold, J., Yao, B., Zeng, W., Chen, Y., 1995a. Deep penetration seismic sounding across the north margin of South China Sea. Journal of Geophysical Research 100 (B11), 22407–22433.
Nissen, S., Hayes, D., Yao, B., Zeng, W., Chen, Y., Nu, X., 1995b. Gravity, heat flow, and seismic constraints on the processes of crustal extension: northern margin of South China Sea. Journal of Geophysical Research 100 (B11), 22447–22483.
Phinney, R.A., Jurdy, D.M., 1979. Seismic imaging of deep crust. Geophysics 44, 1637–1660.
Poppeliers, C., Levander, A., 2004. Estimation of vertical stochastic scale parameters in the Earth's crystalline crust from seismic reflection data. Geophysical Research Letter 31, L13607. http://dx.doi.org/10.1029/2004GL019538.
Qiu, Y., Gao, S., McNaughton, N., Groves, D., Ling, W., 2000. First evidence of >3.2 Ga continental crust in the Yangtze craton of South China and its implications for Archean crustal evolution and Phanerozoic tectonics. Geology 28, 11–14.
Ren, J.S., Chen, T.Y., Niu, B.G., Liu, Z.G., Liu, F.R., 1990. Tectonic Evolution of the Continental Lithosphere and Metallogeny in Eastern China and Adjacent Areas. Science Press, Beijing, p. 205.
Rodgers, J., 1989. Comments on Mesozoic overthrust tectonics in south China. Geology 17, 671–672.
Rowley, D.B., Ziegler, A.M., Nie, G., 1989. Comment on Mesozoic overthrust tectonics in south China. Geology 17, 394–396.
Ruppel, C., 1995. Extensional processes in continental lithosphere. Journal of Geophysical Research B100, 24187–24215.
Shui, T., 1988. Tectonic framework of the continental basement of southeast China. Science Sinica. Series B 31, 885–896.

Su, W.B., Huff, W.D., Ettensohn, F.R., Liu, X.M., Zhang, J.E., Li, Z.M., 2009. K-bentonite, black-shale and flysch successions at the Ordovician–Silurian transition, South China: possible sedimentary responses to the accretion of Cathaysia to the Yangtze Block and its implications for the evolution of Gondwana. Gondwana Research 15 (1), 111–130.
Teng, J.W., Zhang, Z.J., Wang, G.J., 2001a. The Rayleigh wave dispersion and three dimensional velocity structure in continent and its margin of Southeast China. Chinese Journal of Geophysics — Chinese edition 44 (5), 663–677.
Teng, J.W., Wang, G.J., Zhang, Z.J., Hu, J.F., 2001b. Three-dimensional S-wave velocity structure of the South mainland and the southern extension of the Tan-Lu fault zone. Chinese Science Bulletin 45 (23), 2492–3497.
Thybo, H., Nielsen, C.A., 2009. Magma-compensated crustal thinning in continental rift zones. Nature 457 (12). http://dx.doi.org/10.1038/nature07688.
Thybo, H., Maguire, P.K.H., Birt, C., Perchuc, E., 2000. Seismic reflectivity and magmatic underplating beneath the Kenya Rift. Geophysical Research Letter 27 (17), 2745–2748.
Tubía, J.M., Hongn, F.D., Aranguren, A., Vegas, N., 2012. Inversion tectonics in the Pre-andean basement of the Sierra de Cachi (Salta, Argentina). Abstracts of 2012 EGU annual meeting.
van Avendonk Harm, J.A., 2004. Slowness-weighted diffraction stack for migrating wide-angle seismic data in laterally varying media. Geophysics 69 (4), 1046–1052.
Vidale, J., 1988. Finite-difference calculation of travel-times. Bulletin of Seismological Society of America 78, 2062–2076.
Wang, E.K., Liu, C., 1992. Is the Cathaysia a unified block? Geology of collisional orogenic belts in Early Mesozoic in Fujian and Guangdong. In: Li, J.L. (Ed.), Study on the Texture and Evolution of the Oceanic and Continental Lithosphere in Southeastern China. Chinese Science and Technology Press, Beijing, pp. 96–105.
Wang, Y.J., Fan, W., Guo, F., Peng, T., Li, C., 2003. Geochemistry of Mesozoic mafic rocks adjacent to the Chenzhou-Linwu fault, south China: implications for the lithospheric boundary between the Yangtze and Cathaysia blocks. International Geology Review 45, 263–286.
Wang, Y.J., Fan, W., Zhang, Y., Guo, F., Zhang, H.F., Peng, T., 2004. Geochemical, 40Ar/39Ar geochronological and Sr–Nd isotopic constraints on the origin of Paleoproterozoic mafic dikes from the southern Taihang Mountains and implications for the ca. 1800 Ma event of the North China Craton. Precambrian Research 135, 55–77.
Wang, Y.J., Fan, W.M., Peng, T.P., Zhang, H.F., Guo, F., 2005. Nature of the Mesozoic lithospheric mantle and tectonic decoupling beneath the Dabie Orogen, Central China: evidence from 40Ar/39Ar geochronology, elemental and Sr–Nd–Pb isotopic compositions of Mesozoic mafic rocks. Chemical Geology 220, 165–189.
Wang, Y.J., Fan, W.M., Cawood, P.A., Ji, S.C., Peng, T.P., Chen, X.Y., 2007. Indosinian high-strain deformation for the Yunkaidashan tectonic belt, South China: kinematics and 40Ar/39Ar geochronological constraints. Tectonics 26, TC6008. http://dx.doi.org/10.1029/2007TC002099.
Wang, Y.J., Zhang, F.F., Fan, W.M., Zhang, G.W., Chen, S.Y., Cawood, P.A., Zhang, A.M., 2010. Tectonic setting of the South China Block in the early Paleozoic: resolving intracontinental and ocean closure models from detrital zircon U–Pb geochronology. Tectonics 29. http://dx.doi.org/10.1029/2010TC002750.
Wang, Y.J., Zhang, A.M., Fan, W.M., Zhao, G.C., Zhang, G.W., Zhang, Y.Z., Zhang, F.F., Li, S.Z., 2011. Kwangsian crustal anatexis within the eastern South China Block: geochemical, zircon U–Pb geochronological and Hf isotopic fingerprints from the gneissoid granites of Wugong and Wuyi–Yunkai Domains. Lithos 127, 239–260.
Wang, Y.J., Fan, W.M., Zhang, G.W., Zhang, Y.H., 2012. Phanerozoic tectonics of the South China Block: Key observations and controversies. Gondwana Research. http://dx.doi.org/10.1016/j.gr.2012.02.019.
Wei, S., Teng, J., Wang, Q., Zhu, Z., 1990. Crust and Mantle Structure in the East China. China Science Press.
Wernicke, B.P., 1985. Uniform-sense normal simple shear of the continental lithosphere. Canada Journal of Earth Sciences 22, 108–125.
Wong, J., Sun, M., Xing, G.F., Li, X.H., Zhao, G.C., Wong, K., Wu, F.Y., 2011. Zircon U–Pb and Hf isotopic study of Mesozoic felsic rocks from eastern Zhejiang, South China: geochemical contrast between the Yangtze and Cathaysia blocks. Gondwana Research 19 (1), 244–259.
Wyllie, M.R.J., Gregory, A.R., Gardner, L.W., 1956. Elastic wave velocities in heterogeneous and porous media. Geophysics 21, 41–70.
Xiong, S.B., Liu, H.B., Wang, Y.X., Yin, Z.X., Teng, J.W., Hu, H.X., 2002. A study on velocity distribution in upper crust and tectonics of basement and cover in South China. Chinese Journal of Geophysics 45 (6), 784–791 (in Chinese).
Xu, S.T., Sun, S., Li, J.L., Jiang, L.L., Chen, G.B., Shi, Y.H., 1993. Lantian structural window. Science Geologica Sinica 2, 105–116.
Yan, P., Zhou, D., Liu, Z., 2002. A crustal structure profile across the northern continental margin of South China Sea. Tectonophysics 338, 1–21.
Yan, Y.F., Wang, G.J., Zhang, Z.J., 2004. The gravity field and deep crust structure in southeast continent of China. Acta Geologica Sinica 78 (6), 1235–1244.
Yang, Z.Y., Chen, Y.Q., Wang, H.Z., 1986. The Geology of China. Clarendon, Oxford, p. 303.
Yao, J.L., Shu, L.S., Santosh, M., 2011. Detrital zircon U–Pb geochronology, Hf-isotopes and geochemistry — New clues for the Precambrian crustal evolution of Cathaysia Block, South China. Gondwana Research 20 (2–3), 553–567.
Yin, A., Nie, S.Y., 1993. An indentation model for the north and south China collision and the Tan-Lu and Honam fault systems, Eastern Asia. Tectonics 4, 801–813.
Yin, Z.X., Lai, M.H., Xiong, S.B., et al., 1999. Crustal structure and velocity distribution from deep seismic sounding along the profile of Lianxian-Boluo-Gangkou in south China. Chinese Journal of Geophysics 42 (3) (in Chinese).
Yuan, X.C., Zuo, Y., Cai, X.L., Zhu, J.S., 1989. The structure of the lithosphere and the geophysics in the South China Plate. Progress on Geophysics in China in the 1980s. Editorial Board of Bulletin of Geophysics, Beijing, pp. 243–249 (in Chinese and with English abstract).
Zeng, H., Zhang, Q., Li, Y., Liu, J., 1997. Crustal structure inferred from gravity anomalies in South China. Tectonophysics 283, 189–203.
Zhang, Z.J., Wang, Y.H., 2007. Crustal structure and contact relationship revealed from deep seismic sounding data in South China. Physics of the Earth Planetary and Interiors 165, 114–126.
Zhang, Z.M., Liou, J.G., Coleman, R.G., 1984. An outline of the plate tectonics of China. Geological Society of America Bulletin 95, 295–312.
Zhang, L.G., Wang, K.F., Chen, Z.S., Liu, J.X., Yu, G.X., Wu, K.L., Lan, J.Y., 1994. On Cathaysia: evidence from lead isotope study. Geology Reviews 3, 200–208.
Zhang, Z.J., Wang, G.J., Teng, J.W., Klemperer, S.L., 2000. CDP mapping to obtain the fine structure of crust and upper mantle: an example in the Southeastern China. Physics of the Earth Planetary and Interiors 122, 131–144.
Zhang, Z.J., Badal, J., Li, Y., Chen, Y., Yang, L.Q., Teng, J.W., 2005. Crust–upper mantle seismic velocity structure across Southeastern China. Tectonophysics 395, 137–157.
Zhang, Z.J., Zhang, X., Badal, J., 2008. Composition of the crust beneath southeastern China derived from an integrated geophysical data set. Journal of Geophysical Research 113, B04417. http://dx.doi.org/10.1029/2006JB0.
Zhang, Z.J., Teng, J.W., Badal, J., Liu, E.R., 2009a. Construction of regional and local seismic anisotropic structures from wide-angle seismic data: crustal deformation in the southeast of China. Journal of Seismology 13 (2), 241–252. http://dx.doi.org/10.1007/s10950-008-9124-0.
Zhang, Z.J., Liu, Y.F., Zhang, S.F., Zhang, G.C., Fan, W.M., 2009b. Crustal P-wave velocity structure and layering beneath Zhujiangkou-Qiongdongnan basins, the northern continental margin of South China Sea. Chinese Journal of Geophysics — Chinese edition 52 (10), 2461–2471. http://dx.doi.org/10.3969/j.issn.0001-5733.2009.10.005.
Zhang, Z.J., Liu, Y.F., Zhang, S.F., Fan, W.M., Chen, L., 2010. The depth-dependence of crustal extension beneath Qiongdongnan basin area and its tectonic implications. Chinese Journal of Geophysics — Chinese edition 53 (1), 57–66.
Zhang, Z.J., Yang, L., Teng, J., Badal, J., 2011a. An overview of the earth crust under China. Earth-Science Reviews 104, 143–166. http://dx.doi.org/10.1016/j.earscirev.2010.10.003.
Zhang, Z.J., Chen, Q.F., Bai, Z.M., Chen, Y., Badal, J., 2011b. Crustal structure and extensional deformation of thinned lithosphere in Northern China. Tectonophysics 508, 62–72.
Zhang, Z.J., Wu, J., Deng, Y.F., Teng, J.W., Zhang, X., Chen, Y., Panza, G., 2012. Lateral variation of the strength of lithosphere across the eastern North China Craton: new constraints on lithospheric disruption. Gondwana Research. http://dx.doi.org/10.1016/j.gr.2012.03.006.
Zhao, A.H., Zhang, Z.J., Teng, J.W., 2004. Minimum travel time tree algorithm for seismic ray tracing: improvement in efficiency. Journal of Geophysics and Engineering 1 (4), 245–251.
Zhao, B., Zhang, Z., Bai, Z.M., Zhang, Z.J., Badal, J., accepted for publication. Shear velocity and Vp/Vs ratio structure of the crust beneath the southern margin of South China continent. Journal of Asian Earth Sciences.
Zhao, B., Bai, Z.M., Xu, T., Badal, J., in preparation. Composition of the crust beneath South China with integrated geophysical dataset. Journal of Geophysics and Engineering.
Zhou, X., Li, W., 2000. Origin of Late Mesozoic igneous rocks in Southeastern China: implications for lithospheric subduction and underplating of mafic magmas. Tectonophysics 326, 269–287.
Zhou, M.F., Yan, D.P., Kennedy, A.K., Li, Y.Q., Ding, J., 2002. SHRIMP U–Pb zircon geochronological and geochemical evidence for Neoproterozoic arcmagmatism along the western margin of the Yangtze Block South China. Earth and Planetary Science Letters 196, 51–67.
Zhu, J.S., Cao, J., Cai, X., Yan, Z., Cao, X., 2002. High resolution surfacewave tomography in East Asia and West Pacific marginal seas. Chinese Journal of Geophysics — Chinese edition 45 (5), 679–698.